PGC PUBLISHING

Paterson, J.T. and Cloos M., 2005 - Grasberg Porphyry Cu-Au Deposit, Papua, Indonesia: 2. Pervasive Hydrothermal Alteration; *in Porter, T.M. (Ed.), Super Porphyry Copper & Gold Deposits: A Global Perspective*; PGC Publishing, Adelaide, v. 2, pp 331-355.

GRASBERG PORPHYRY Cu-Au DEPOSIT, PAPUA, INDONESIA: 2. PERVASIVE HYDROTHERMAL ALTERATION

John T. Paterson and Mark Cloos

Department of Geological Sciences, University of Texas at Austin, USA

Abstract - The Grasberg Igneous Complex (GIC) is host to one of the largest copper and gold porphyry-type ore deposits discovered on Earth. Much of the rock volume in the GIC has been pervasively altered by the infiltration of hot, magmatic fluids. In parts of the deposit, alteration destroyed all igneous phases. Petrography reveals that two zones characterise almost the entire complex at the level of the open pit mine. The 1 km-wide core of the deposit is dominated by biotite + magnetite with an inner ~500 m-wide sub-zone containing andalusite. The exterior annular zone, ~500 m across, is dominated by sericite + anhydrite + pyrite with small amounts of kaolinite. Pockets of rock contain epidote with chlorite in the distal portions of the GIC.

The pattern of hydrothermal alteration indicates an intense episode of pervasive fluid flow post-dated the Main Grasberg Intrusion and predated the Late Kali Intrusion. The overall pattern indicates the interior was hot and acid-producing and the exterior was cooler and acid-consuming. In the core of the GIC, the precipitation of abundant magnetite caused outwards moving fluids to become acidic. In the cooler, outer parts of the complex, these acidic fluids caused the hydrolysis of plagioclase and other minerals into sericite. The cooling of outwards flowing fluids also caused the hydrolysis of SO_2 to H_2S and H_2SO_4 which, in turn, caused the precipitation of sulphide minerals and anhydrite. The overprint of sericite + anhydrite + pyrite upon the biotite + magnetite zone is limited in area and of minor intensity. Compared to most other porphyry copper deposits, the pervasive infiltration of magmatic fluid ended rather abruptly.

Introduction

A concentric pattern of mineralogic zones is such a distinctive feature of copper porphyry deposits that recognition has long been used in the search for porphyry copper-type mineralisation and as a guide for exploration drilling (Lowell, 1995). Pervasive infiltration and hydrothermal alteration that emanates from a point source is the simple explanation for the bullseye pattern of zonation that characterises these deposits. The basic zonation was first recognised by Sales and Meyer (1950), but it was Lowell and Guilbert (1970) who provided an extensive review of porphyry copper systems that focused on the mineralogic commonalties of the alteration zoning. They described the San Manuel-Kalamazoo deposit in the southwestern United States as the type example. In this deposit, a central core of potassic alteration, with a mineral assemblage characterised by quartz, potassium feldspar, and hydrothermal biotite, grades outwards to a phyllic 'shell' of quartz, sericite and pyrite, which in turn grades into a 'shell' of propylitic alteration, characterised by chlorite, epidote, and albite. More irregularly developed, but concentrated on the outer margins is argillic alteration, characterised by quartz, kaolinite, and chlorite. Lowell and Guilbert (1970) proposed that following the intrusion of a stock, the concentric alteration zones form as a result of a continuum of conditions as hot magmatic fluids in the core of the system cool as they move outwards. Gustafson and Hunt (1975) proposed, following a study of the El Salvador deposit in Chile, that magmatic-fluid dominated alteration (potassic alteration) in the core of the deposit grades into alteration that is dominated by meteoric fluid (phyllic alteration, or feldspar-destructive). As the system cools, the hydrothermal system collapses and phyllic alteration is superimposed on the potassic zone. The superposition of alteration zones is reported for many deposits.

Mineralisation in copper porphyry systems arises from two fundamentally different forms of fluid flow (Burnham, 1979; Rose and Burt, 1979), namely: 1) extension fractures with mineral precipitation forming veins, and 2) diffuse infiltration causing pervasive alteration and disseminated mineralisation. It is the diffuse infiltration that defines the concentric zones and involves volumes of rock on the scale of cubic kilometres. To some extent, these processes are overlapping. Most veins are tabular with no obvious alteration of the enclosing wall rocks, but some are accompanied by alteration 'halos' that indicate centimetre-scale infiltration and locally intense alteration of the wall rock.

The Grasberg porphyry Cu-Au deposit, which formed at ~3 Ma, is one of the largest on Earth. A brief discussion of the regional geology and characterisation of the primary

magmatic mineralogy is presented in a companion paper (Paterson and Cloos, this volume). This paper focuses on the pervasive alteration history of the GIC caused by the pervasive infiltration of hydrothermal fluid.

Previous Work on the Grasberg System

Van Nort et al. (1991) presented a general description of the Grasberg Igneous Complex (GIC) and the contained Cu-Au ore body (Fig. 1). MacDonald and Arnold (1994) provided the first detailed examination of magmatic mineralogy, alteration and mineralisation. In their study, they described a genetic model for alteration in which different stages of alteration and associated mineralisation follow the intrusion of the three main magmatic phases: Dalam, Main Grasberg Intrusion (MGI), and Kali (Fig. 2). They proposed that pervasive alteration and disseminated mineralisation in the GIC dominates in the Dalam phase rocks, with an outer zone of phyllic alteration (sericite + quartz + pyrite) that transitions inwards to the core zone of potassic alteration (potassium feldspar + biotite + magnetite). Propylitic alteration (epidote ± chlorite) is limited to the extreme periphery of the GIC and argillic alteration (clays) is only locally developed in the phyllic zone. The authors reported only weak pervasive alteration in the MGI and noted minimal alteration in the Kali.

Previous studies of alteration/mineralisation at the University of Texas at Austin (Penniston-Dorland, 1997; Sapiie, 1998) concentrated upon the pattern and orientation of veins in the open pit mine. A concentric zonation of veining is evident centred on the core of the deposit. Penniston-Dorland (1997) provided an analysis of vein mineralogies, concluding that two main stages of veining occurred: post Dalam and MGI, and post Late Kali Intrusion (LKI). The first stage (confined to the Dalam and MGI) was volumetrically abundant and stockwork-forming (networks of veins indicating a three-dimensional dilatation) in the core of the GIC. Stage 1a magnetite + quartz veining was overprinted by Stage 1b chalcopyrite veining. Stage 2 veining was volumetrically minor, postdated the Late Kali Intrusion, and was chemically distinctive forming biotite with little associated copper sulphide mineralisation. Cross-cutting veins are common, but there are very few veins (<1%) re-opened to become lined with more than one generation of minerals (Sapiie, 1998).

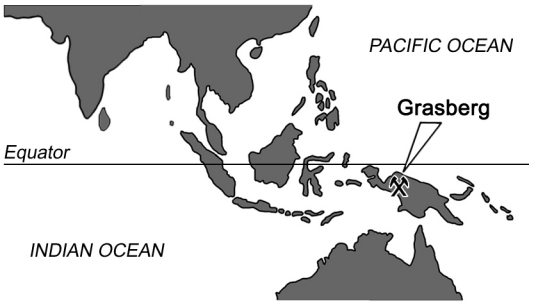

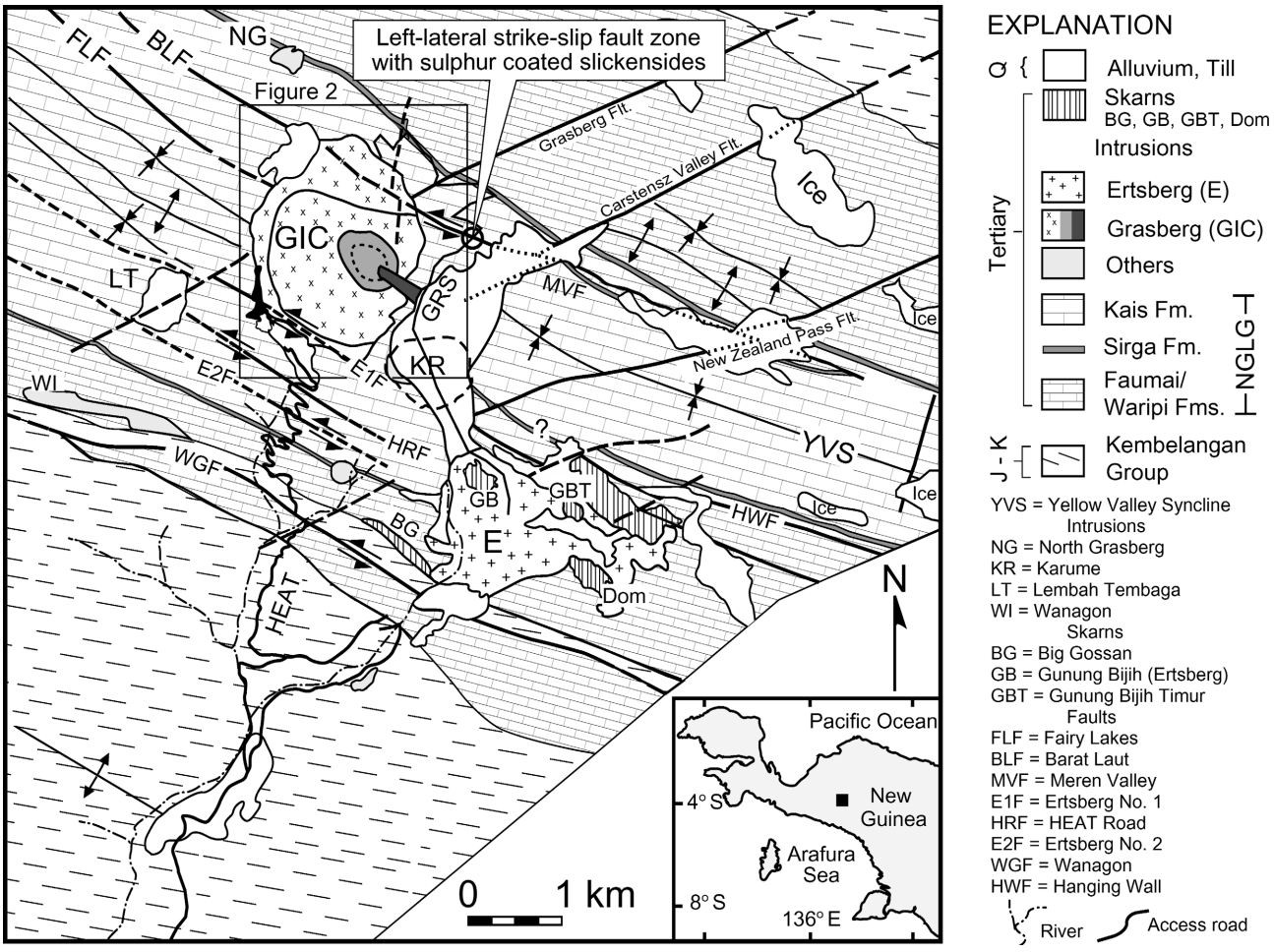

Figure 1: ***Geologic map of Ertsberg Mining District, Papua, Indonesia.***

Millimetre to centimetre-scale sericitic alteration halos are associated with some of the pyrite ± quartz veins. The whitish halos are especially distinct where they cut rock that is black because of abundant magnetite and biotite. Penniston-Dorland (1997) found that geochemical changes in the alteration halos involve the removal of major oxides such as Na_2O, MgO and CaO as well as trace elements such as Cu, Rb and Sr. She concluded that the alteration forming the halos was the result of acid consumption, or of acid attack on the silicate host rock by the pyrite vein-forming fluid. In doing so, she showed that the alteration halos in the GIC have mineralogies very similar to those commonly reported in the phyllic zone of pervasive alteration. In addition, Penniston-Dorland (2001) used cathodoluminescence analysis to show that the quartz veins were the product of a single opening, fluid infiltration and mineral precipitation event.

Sapiie (1998) mapped the pattern of faulting and vein zonation in the open pit mine (Fig. 3). He divided the GIC into three 300°-trending zones dominated by strike-slip faults that cross-cut the veins. Sapiie (1998) concluded that the GIC formed in a 2 km-wide pull-apart, or extensional jog, connecting the Meren Valley and Ertsberg No. 1 left-lateral strike-slip faults. Based upon 1996 mapping in the open pit mine, vein abundance is greatest in a slightly elongated 400 x 500 m zone centred on the MGI. Sapiie (1998) mapped the boundaries of the abundant chalcopyrite veining forming most of the highest grade ore (a stockwork zone of Stage 1b) superimposed upon the quartz-magnetite stockwork of Stage 1a (Fig. 3). Inner and outer limits were mapped for vein populations such as quartz + pyrite + anhydrite and pyrite ± quartz veins with alteration envelopes. Most importantly, he deduced that strike-slip faulting, pull-apart extension and veining were causally related.

In striking contrast to the two-stage model for extension fracturing/veining discussed above, Pollard and Taylor (2002) identified 35 temporally and chemically distinct generations of veining and alteration, several of which were also spatially distinct. Their analysis was based on a 'fan'

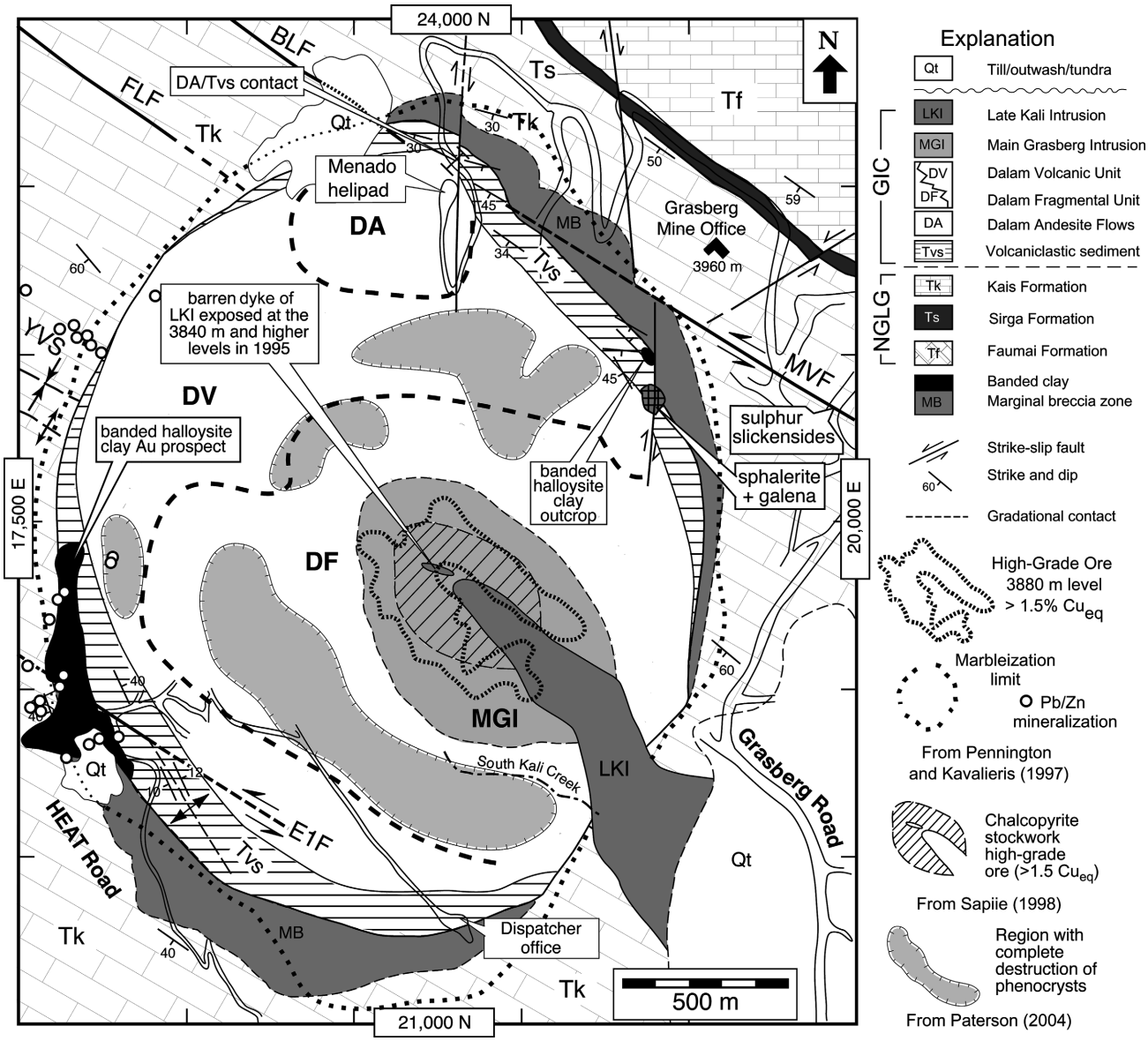

Figure 2: ***Geology of the Grasberg Igneous Complex (GIC) at the ~3900 m elevation.*** Modified from Suwardy (1995) and Sapiie (1998). The Meren Valley Fault (MVF) and Ertsberg #1 Faults (E1F) are left-lateral strike-slip faults. Sapiie (1998) concluded the GIC was emplaced into a pull-apart connecting these fault zones.

of drill cores representing a vertical section trending NE-SW through the centre of the deposit from approximately 2600 to 4000 m. Thus, at the beginning of this investigation there were two distinct pictures for alteration and mineralisation: two distinct alteration/mineralisation events and the Pollard and Taylor perspective of many pulses of chemically distinct fluid flow and associated mineralisation.

This study focuses on evaluating the pervasive alteration and disseminated mineralisation in the Grasberg system via the analysis of hand specimens, polished slabs and thin sections of a suite of 225 samples collected in the open pit mine between 1994 to 2002. The samples were located between the elevations of 3700 m and 4200 m, most between 3800 m to 4100 m. Because the Grasberg was a hill prior to mining, the effect of sampling over time resulted in a suite that constitutes a roughly horizontal cross section at ~3900 m elevation. These samples are the basis for constructing a set of maps that depict mineralogic and textural variations of pervasive alteration in the GIC.

Hydrothermal Mineralogy

The petrographic study of hydrothermally altered rocks is difficult owing to the fine grain size produced by pervasive alteration. Petrographic analysis revealed cryptic micro-textures that were used as the basis for selecting samples for standard x-ray diffraction and electron microprobe analysis to confirm the identification of fine-grained minerals. See Paterson (2004) for analytical details.

Hand Specimen Observations

The magmatic mineralogy of the igneous units in the GIC is summarised in Table 1. From the fresh LKI through to the highly altered Dalam phase rocks, photographs of polished slabs (Fig. 4) illustrate the nature of pervasive alteration which is locally severe enough to completely destroy all magmatic phenocrysts (shaded regions on Fig. 2).

Hydrothermal Biotite

Biotite comprises 3 to 25%, typically 15%, of the magmatic phenocryst population (Paterson and Cloos, this volume) and is a major alteration product. Although in principle differentiation could be difficult, hydrothermal biotite is petrographically very distinct from magmatic biotite due to the marked contrast in morphology. Phenocrystic (magmatic) biotite commonly has a euhedral shape with crystal sizes typically 0.5 to 2 mm across. Groundmass magmatic biotite occurs as solitary grains typically about 0.2 mm across. Hydrothermal biotite, in striking contrast,

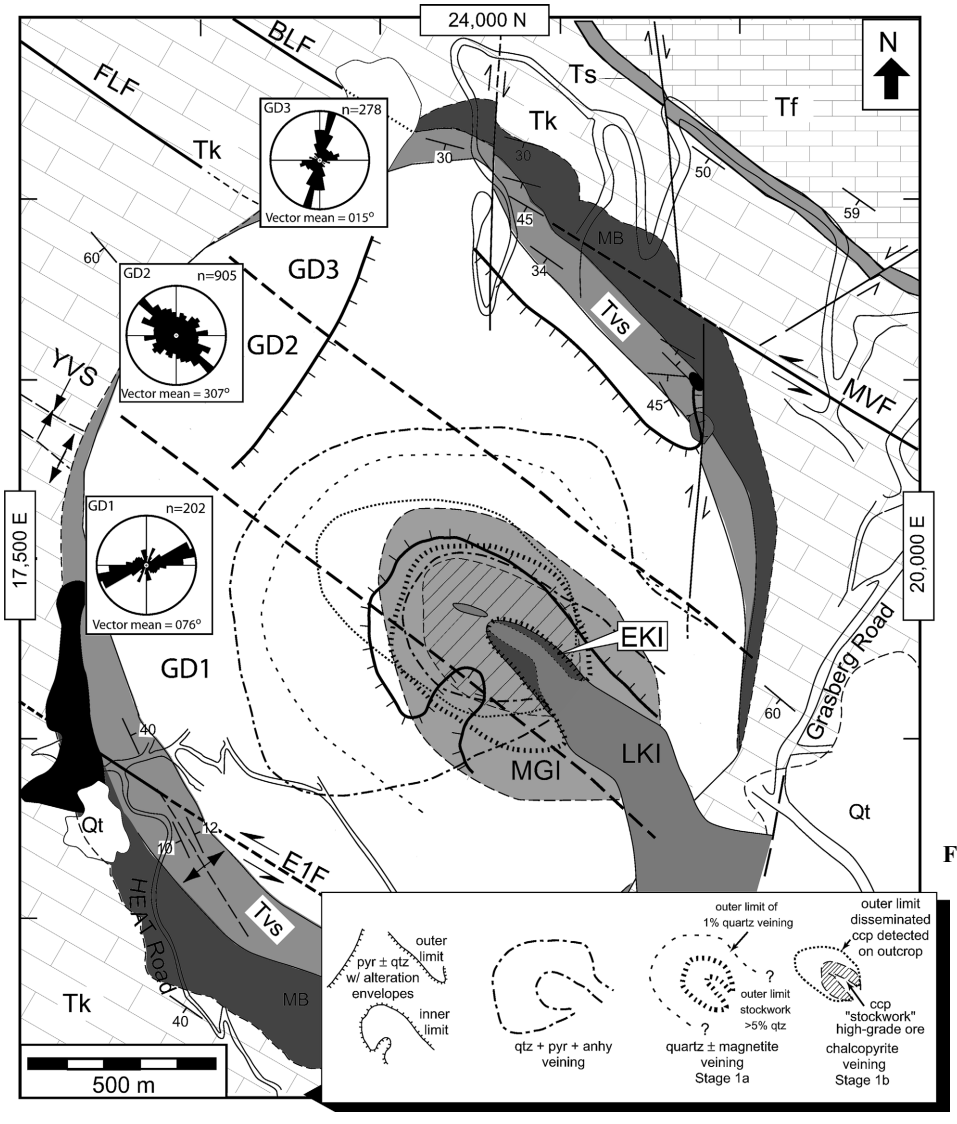

Figure 3: ***Vein type and density, and structural domains*** identified by Sapiie (1998). Grasberg Structural Domain 1, GD1, is dominated by 76˚ trending left-lateral strike-slip faults. GD2 is dominated by 307˚ trending left-lateral strike-slip faults. GD3 is dominated by 15˚ trending, right-lateral strike slip faults.

Table 1: ***Magmatic mineralogy of the igneous units in the Grasberg Igneous Complex***

youngest	**Late Kali Intrusion (LKI)**	
	phenocrysts	plagioclase (20% to 65%) + biotite (10% to 20%) + hornblende (3% to 15%) ± clinopyroxene (altered to actinolite) (~2%)
	groundmass	potassium feldspar (10% to 30%), quartz (10% to 30%), biotite (~5%), albitic plagioclase (~5%), magnetite (~2%) and apatite (tr.)
	texture	porphyritic: ~100x variation in grain size
	Early Kali Intrusion (EKI)	
	phenocrysts	plagioclase (20% to 65%) + biotite (10% to 20%)
	groundmass	potassium feldspar (10% to 30%), quartz (10 to 30%), biotite (~10%), albitic plagioclase (~5%), and apatite (tr.)
	texture	porphyritic: ~100x variation in grain size
	Main Grasberg Intrusion (MGI)	
	phenocrysts	plagioclase (20% to 40%) + biotite (5% to 25%) + hornblende (3% to 15%) + clinopyroxene (altered to actinolite) (~5%)
	groundmass	potassium feldspar (~15%), quartz (~15%), biotite (~5%), albitic plagioclase (~5%), and apatite (tr.)
	texture	comparatively equigranular: ~10x variation in grain size
	Dalam Andesite (DA)	
	phenocrysts	plagioclase (10% to 35%) + biotite (5% to 25%) + hornblende (3% to 15%)
	groundmass	potassium feldspar (~10%), quartz (~20%), biotite (~10%), albitic plagioclase (~5%), and apatite (tr.)
	texture	porphyritic: ~100x variation in grain size
	Dalam Volcanic/Dalam Fragmental (DV/DF)	
	phenocrysts	plagioclase (up to 45%) and biotite (3% to 20%) +/- hornblende (< 2%)
	groundmass	thoroughly altered in almost all samples, may have been glassy, apatite (tr.)
oldest	**texture**	brecciated, with broken plagioclase crystals

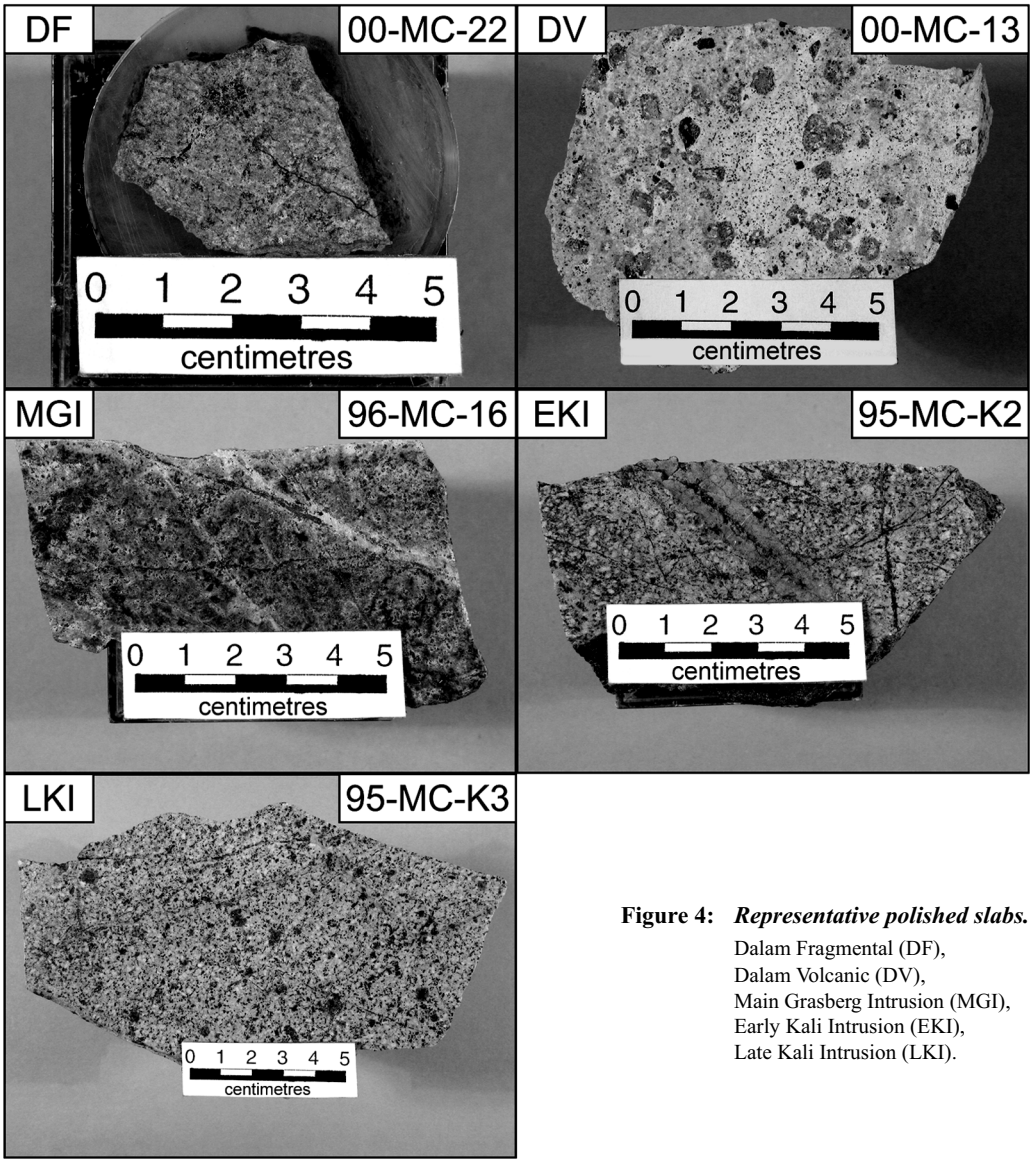

Figure 4: ***Representative polished slabs.***
Dalam Fragmental (DF),
Dalam Volcanic (DV),
Main Grasberg Intrusion (MGI),
Early Kali Intrusion (EKI),
Late Kali Intrusion (LKI).

occurs as "shreddy" aggregates of grains that are most commonly smaller than 0.1 mm across. Similar habits for biotite are reported in many copper-porphyry systems (Creasey, 1966; Dilles and Einaudi, 1992).

Hydrothermal biotite is abundant in the core, but absent in the outer portions of the GIC (Fig. 5). The Late Kali (LKI) has little (typically trace to 5%) hydrothermal biotite compared to the Early Kali (EKI) (5 to 15%). This indicates that the emplacement of the LKI occurred after pervasive hydrothermal alteration had essentially ended. In the interior of the GIC, near the northwestern border of the MGI and DF, trace amounts of green biotite is present as replacement rims on hydrothermal, brown biotite. Petrographically it looks similar to green phlogopite.

Pseudomorphic relationships indicate much of the hydrothermal brown biotite formed from replacement of plagioclase, hornblende and biotite phenocrysts. It is commonly intimately associated with magnetite. The infiltration of potassic, metal-rich brines can account for the alteration. The products are acidic, Ca-rich, fluids.

Idealised end-member reaction chemistries (with FM= Fe, Mg) for these pseudomorphic reactions are:

biotite replacing plagioclase,

$$CaAl_2Si_2O_8 + 4SiO_4 + 2KCl + 6FMCl_2 + 8H_2O \rightarrow 2KFM_3AlSi_3O_{10}(OH)_2 + CaCl_2 + 12HCl \quad (1a)$$

$$NaAlSi_3O_8 + KCl + 3FMCl_2 + 4H_2O \rightarrow KFM_3AlSi_3O_{10}(OH)_2 + NaCl + 6HCl \quad (1b)$$

biotite replacing calcic hornblende,

$$Ca_2FM_4AlSi_7AlO_{22}(OH)_2 + 2KCl + 2FMCl_2 + 2H_2O \rightarrow 2KFM_3Si_3AlO_{10}(OH)_2 + 2CaCl_2 + SiO_2 + 4HCl \quad (2)$$

Microprobe analysis shows brown hydrothermal biotite has a higher Mg content than magmatic biotite. The idealised exchange reaction below also accounts for the intimate association of magnetite with replacement biotite:

$$KFe_3AlSi_3O_{10}(OH)_2 + 6FeCl_3 + 3MgCl_2 + 12H_2O \rightarrow KMg_3AlSi_3O_{10}(OH)_2 + 3Fe_3O_4 + 24HCl \quad (3)$$

The compositional difference between magmatic and hydrothermal biotite (Fe, Mg, Ti) is relatively small (Fig. 6). This is interpreted to indicate the thermal and chemical conditions under which both types formed were similar.

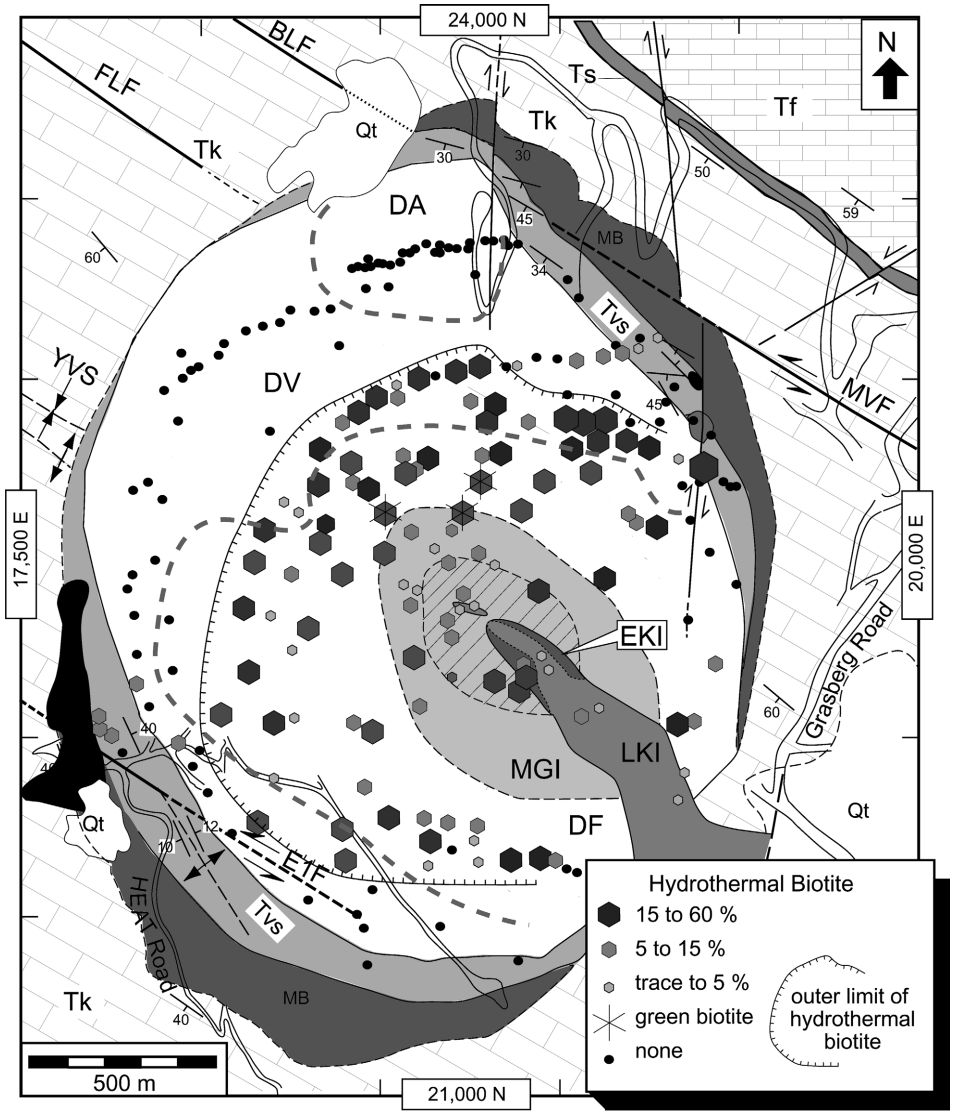

Figure 5: ***Distribution and abundance of hydrothermal biotite.***

Magmatic biotite equilibrated with a melt. Hydrothermal biotite in the core of the GIC equilibrated with a magmatic fluid that was not substantially cooler than the temperature of total magmatic solidification.

Green biotite crystals were only coarse enough for analysis in one sample (94-MC-D2). They differ markedly in composition from magmatic biotite or hydrothermal brown biotite. Using normalisation schemes for biotite (Yavuz and Oztas, 1997), the brown biotite is relatively Mg and Ti-rich whereas the green biotite is relatively Al and Fe^{3+}-rich. Therefore, the green biotite crystals appear to record equilibration with either a Mg- and Ti-poor fluid (the latter a strong indicator of lower temperature) and/or a more oxidised fluid during the waning of the hydrothermal system. An important feature of the occurrence of green biotite is that it is localised to near the centre of the GIC.

Sericite (Fine-Grained Muscovite)

Unlike hydrothermal biotite, there is no magmatic muscovite. Fine-grained hydrothermal muscovite (sericite) is typically very easy to identify in thin section, but in large parts of many thin sections, sericite is below petrographic resolution. Sericite is typically associated with pyrite, anhydrite/gypsum/porosity, and quartz.

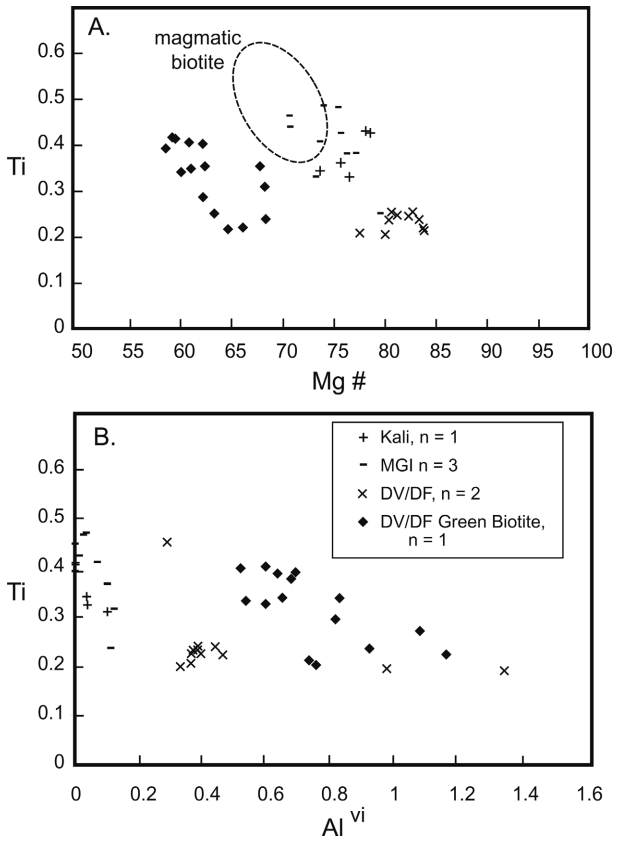

Figure 6 (above): ***Composition of shreddy, hydrothermal biotite.***

A. Ti versus Mg # = Mg/Fe+Mg.

B. Ti versus Al in six-fold coordination. Ti and Al cations calculated on basis of 44 negative charges.

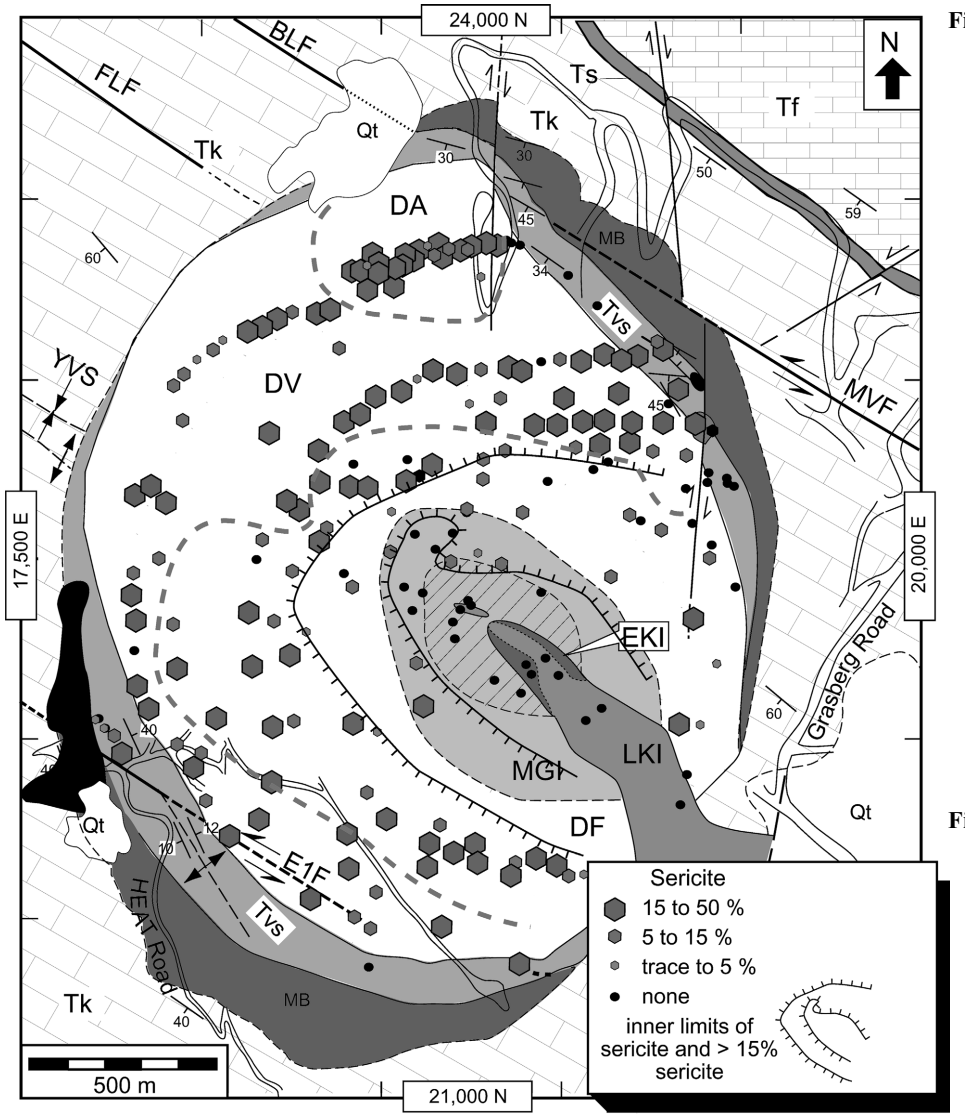

Figure 7 (left): ***Distribution and abundance of sericite*** (fine-grained muscovite).

In marked contrast to the pattern of hydrothermal biotite, which is only present in the interior of the GIC, sericite is, with the exception of bleached alteration halos along pyrite ± quartz veins, only present in the outer portion of the GIC (Fig. 7). Noticeably, there are also regions, or pockets, in the exterior of the GIC where sericite is minor or absent and the mineral assemblage is dominated by epidote ± chlorite (see below). Comparison of Figs. 5 and 7 shows the portion of the GIC dominated by sericite is an annular region (with an inner radius of approximately 500 m) in which hydrothermal biotite is minor or absent.

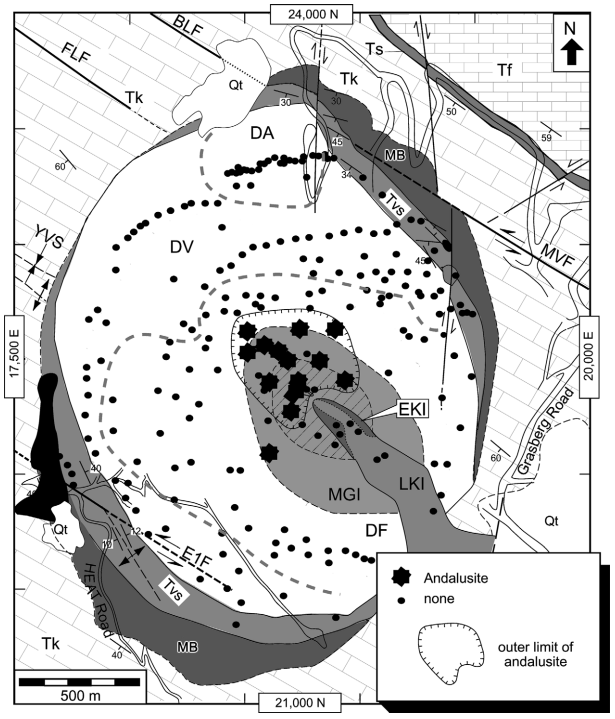

Figure 8: ***Distribution of andalusite.*** Note the occurrences are isolated to the interior of the Grasberg Igneous Complex.

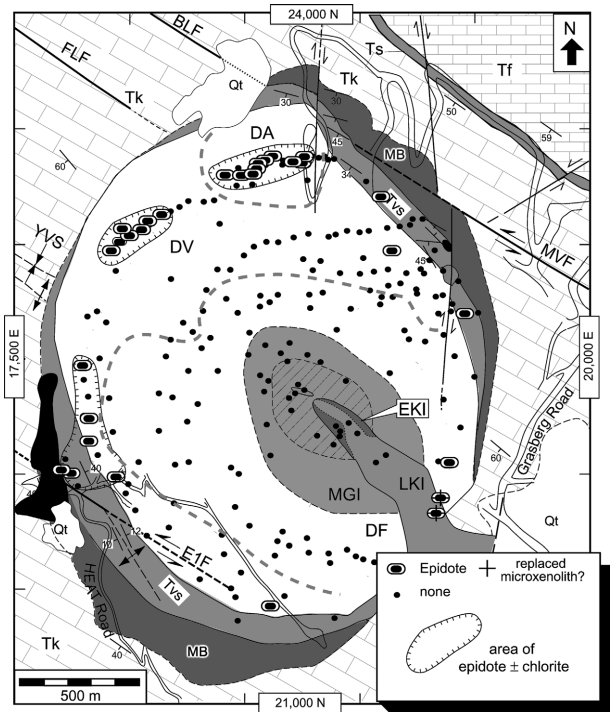

Figure 9: ***Distribution of epidote.*** Note the occurrences are isolated to the margins of the Grasberg Igneous Complex.

Sericite commonly occurs as a pseudomorphic replacement of groundmass potassium feldspar, and of plagioclase and biotite phenocrysts. Idealised reactions (with FM=Fe, Mg) for the replacements are all acid-consuming:

sericite replacing potassium feldspar;

$$3KAlSi_3O_8 + 2HCl \rightarrow KAl_3Si_3O_{10}(OH)_2 + 6SiO_2 + 2KCl \quad (4)$$

sericite replacing plagioclase,

$$3CaAl_2Si_2O_8 + 2KCl + 4HCl \rightarrow 2KAl_3Si_3O_{10}(OH)_2 + 3CaCl_2 \quad (5a)$$

$$3NaAlSi_3O_8 + KCl + 2HCl \rightarrow KAl_3Si_3O_{10}(OH)_2 + 6SiO_2 + 3NaCl \quad (5b)$$

sericite and pyrite replacing magmatic biotite,

$$3KFe_3AlSi_3O_{10}(OH)_2 + 2HCl + 15H_2S + 3SO_2 \rightarrow KAl_3Si_3O_{10}(OH)_2 + 2KCl + 9FeS_2 + 6SiO_2 + 18H_2O \quad (6a)$$

$$3KMg_3AlSi_3O_{10}(OH)_2 + 20HCl \rightarrow KAl_3Si_3O_{10}(OH)_2 + 2KCl + 9MgCl_2 + 6SiO_2 + 12H_2O \quad (6b)$$

Andalusite

Andalusite was discovered in the GIC by Penniston-Dorland (1997). The grain size is typically less than 30 microns. Petrographic identification of andalusite is based on the high relief and birefringence and confirmed with energy-dispersive analysis on the electron microprobe.

Fig. 8 shows that andalusite is only present in the interior of the GIC. Andalusite was not found in any of the Kali samples. It is spatially associated with magnetite and hydrothermal biotite. No replacement reaction is apparent for andalusite and most appears to be in the groundmass.

It is hypothesised that andalusite is a replacement of potassium feldspar and plagioclase. The idealised reactions are:

andalusite replacing potassium feldspar;

$$2KAlSi_3O_8 + 2HCl \rightarrow Al_2SiO_5 + 2KCl + 5SiO_2 + H_2O \quad (7)$$

andalusite replacing plagioclase;

$$CaAl_2Si_2O_8 + 2HCl \rightarrow Al_2SiO_5 + CaCl_2 + SiO_2 + H_2O \quad (8a)$$

$$2NaAlSi_3O_8 + 2HCl \rightarrow Al_2SiO_5 + 2NaCl + 5SiO_2 + H_2O \quad (8a)$$

Thermodynamic modeling (Paterson, 2004) indicates that andalusite is a high-temperature alumino-silicate alteration product (T >425°C). The distribution of andalusite indicates the centre of highest-temperature pervasive alteration was located about 250 m to the northwest of the tip of the wedge-shaped Kali intrusion.

Epidote

Epidote is relatively easy to identify petrographically owing to its pale yellow-green colour and high relief. Fig. 9 shows epidote occurs near the edges of the deposit, in patches that are surrounded by rock altered to sericite and pyrite. Moreover, the occurrences of epidote is also discontinuous at the cm scale of thin sections.

Epidote-bearing samples are associated with chlorite and albite, a common low-temperature (~200 to 300°C) greenschist facies mineral assemblage. The occurrence of epidote delineates portions of the GIC that underwent more of an isochemical thermal metamorphism rather than one of pervasive invasion by chemically destructive acidic fluids.

Pyrite

Pyrite is easily identifiable in hand specimen and reflected light microscopy owing to its pale-yellow colour. It is found with euhedral crystal shapes, but most typically occurs as grain aggregates associated with sericite.

In a limited band, pyrite also occurs (trace to 1%) as overgrowths, intergrowths, or replacements of magnetite (discussed below).

Fig. 10 shows pyrite is disseminated throughout the outer portions of the GIC. It is abundant (5% to 10%) in an annular-shaped region roughly congruent with the greatest abundances of sericite (compare with Fig. 8).

An idealised reaction for the precipitation of pyrite from hydrothermal fluid is:

$$3FeCl_2 + 5H_2S + SO_2 \rightarrow 3FeS_2 + 6HCl + 2H_2O \qquad (9)$$

The precipitation of pyrite requires the presence of reduced sulphur and generates acid.

Magnetite

Magnetite is readily identifiable in reflected light microscopy owing to its characteristic steel-grey colour. Magnetite does not exhibit a characteristic crystal shape and is only unambiguously identifiable as a member of the magmatic assemblage in the most unaltered portions of the Late Kali (Paterson and Cloos, this volume) where it comprises 1% to 2% of the rock.

There is a fundamental problem of differentiating magmatic magnetite from hydrothermal magnetite. In the portions of the Early Kali, MGI, and Dalam where magnetite veins are common, the abundance of disseminated magnetite is generally 5% to 10% and locally greater.

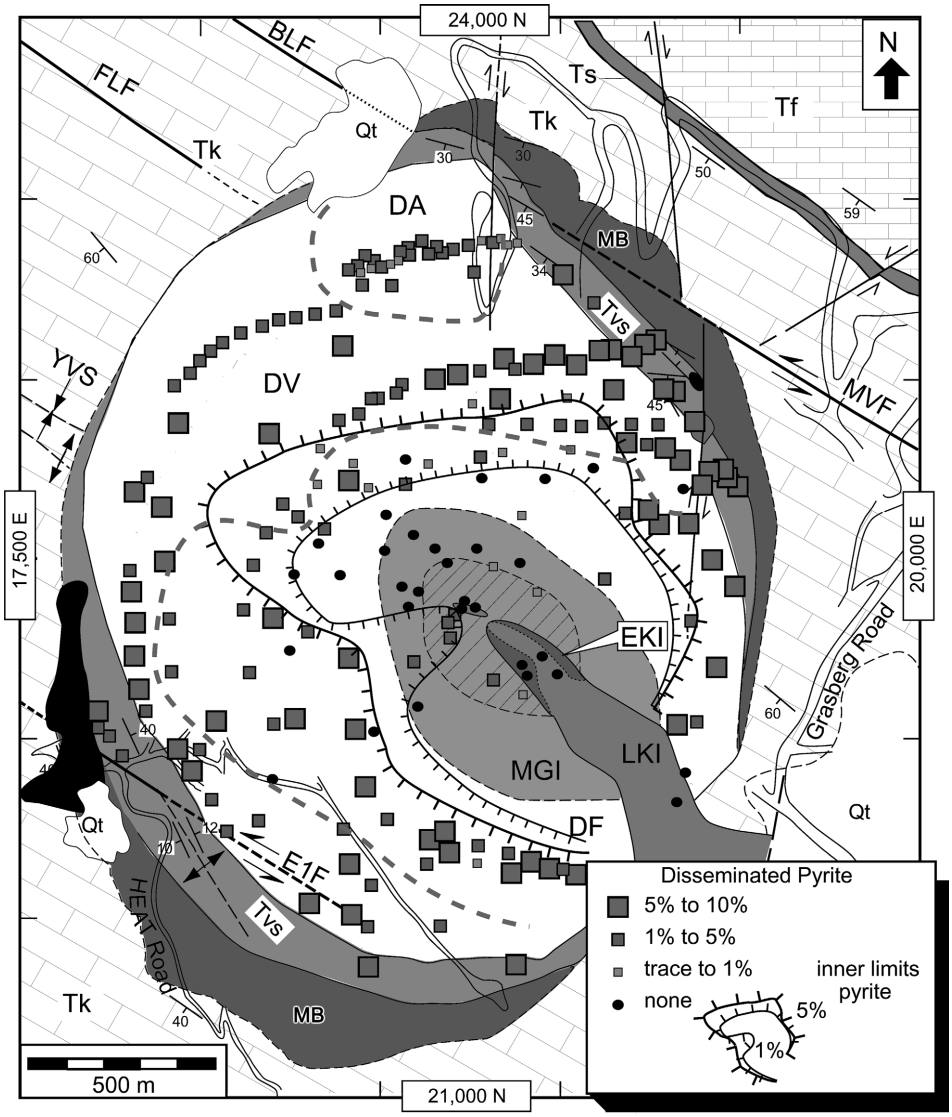

Figure 10: ***Distribution and abundance of disseminated pyrite.*** Note pyrite is lacking in some samples from the interior of the complex.

Fig. 11 shows disseminated magnetite is abundant in the core of the GIC and has only scattered occurrences in the exterior, where pyrite is abundant. Where abundant, magnetite is intimately associated with hydrothermal biotite. The minor, scattered occurrences in the periphery of the deposit may be relict igneous magnetite. The biotite + magnetite association is locally overprinted by the sericite + anhydrite + pyrite assemblage (discussed below).

An idealised reaction for the precipitation of hydrothermal magnetite from oxidising (high Fe^{+3}/Fe^{+2} ratio) hydrothermal fluid are:

$$2FeCl_3 + FeCl_2 + 4H_2O \rightarrow Fe_3O_4 + 8HCl \quad (10)$$

The precipitation of magnetite causes fluid to become acidic. As magnetite is abundant in the core of the GIC, the acidity must have increased substantially as fluid moved outwards and upwards.

Chalcopyrite

Chalcopyrite is the dominant ore mineral in the open pit mine. Disseminated chalcopyrite has no distinctive crystal shape and has abundances as great as 3%. Even trace occurrences of chalcopyrite are readily detectable in thin section because of its distinctive yellow-gold colour.

At the ~3900 m elevation, the highest-grade ore occurs in a zone that is approximately 500 m-long by 400 m-wide. This ore zone contains a stockwork of chalcopyrite veins (marked with a hachured pattern on Fig. 13) that are locally up to 1 to 2 centimetres thick. The limit of disseminated chalcopyrite occurrence is at about 750 m from the centre. Notably, Fig. 12 shows that disseminated chalcopyrite is scarce in the part of the MGI where chalcopyrite veining is most abundant.

Chalcopyrite has a spatial association with both disseminated magnetite and hydrothermal biotite, and was precipitated at higher temperatures than most of the pyrite. Idealised reactions for the precipitation of chalcopyrite from hydrothermal fluid are:

$$CuCl_2 + FeCl_2 + 2H_2S \rightarrow CuFeS_2 + 4HCl \quad (11a)$$
$$CuCl + FeCl_3 + 2H_2S \rightarrow CuFeS_2 + 4HCl \quad (11b)$$

As with the precipitation of magnetite, the precipitation of chalcopyrite increases the acidity of the hydrothermal fluids passing through the rocks.

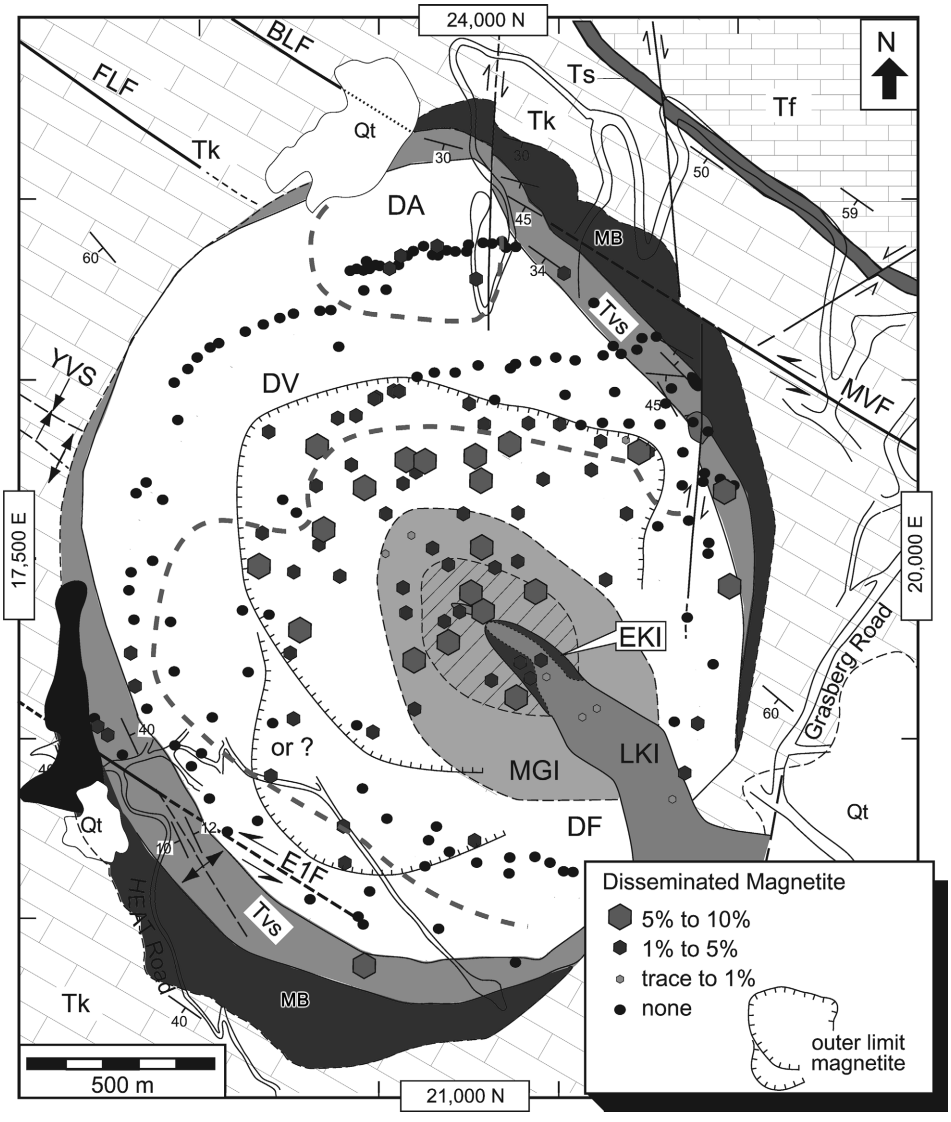

Figure 11: ***Distribution and abundance of disseminated magnetite.*** Note magnetite is not present in many samples from the exterior of the complex.

Anhydrite

Anhydrite has high solubility in ground water, and hence was readily leached as meteoric water invaded the deposit. Consequently, a lack of anhydrite in thin section is not a basis for inferring an original absence from the rock volume. Where anhydrite is dissolved, porosity is generated and its former presence is commonly indicated by very thin rinds of anhydrite/gypsum along the margins of vuggy pores. Anhydrite is very distinct in thin section owing to its excellent cleavage and very high birefringence. It ranges from very small individual grains (<30 microns) to large poly-crystalline patches, locally comprising up to 10% of the rock volume.

Anhydrite (Fig. 13) and vuggy porosity (Fig. 14) occur in an annular region starting about 500 m from the centre of the GIC. Only trace amounts of anhydrite (<1%) were ever present in the interior where hydrothermal biotite and magnetite dominate. Anhydrite appears to have been most abundant at about 750 m from the centre of the GIC and decreases towards the edges. This relationship is particularly pronounced at depth where it is essentially absent from the edges of the GIC and in the Heavy Sulphide Zone (Lambert, 2000).

A comparison between Fig. 13 and Fig. 14 highlights the variable preservation of anhydrite and the effect of ground water dissolution. Anhydrite/gypsum/vuggy porosity, together with sericite and pyrite, define the outer zone of alteration in the GIC.

The character of sulphur species in solution is of utmost importance in determining the mineralogies of alteration. The near-lack of anhydrite in the interior of the deposit requires explanation. Sulphur dioxide (the dominant sulphur phase in magmatic fluids discharged from erupting volcanoes) undergoes hydrolysis in cooling hydrothermal fluids:

$$4H_2O + 4SO_2 \rightarrow H_2S + 3H_2SO_4 \qquad (12)$$

The importance of this reaction was first recognised by Holland (1965) and subsequent studies indicates SO_2 is the dominate sulphur species exsolved from cooling magmas.

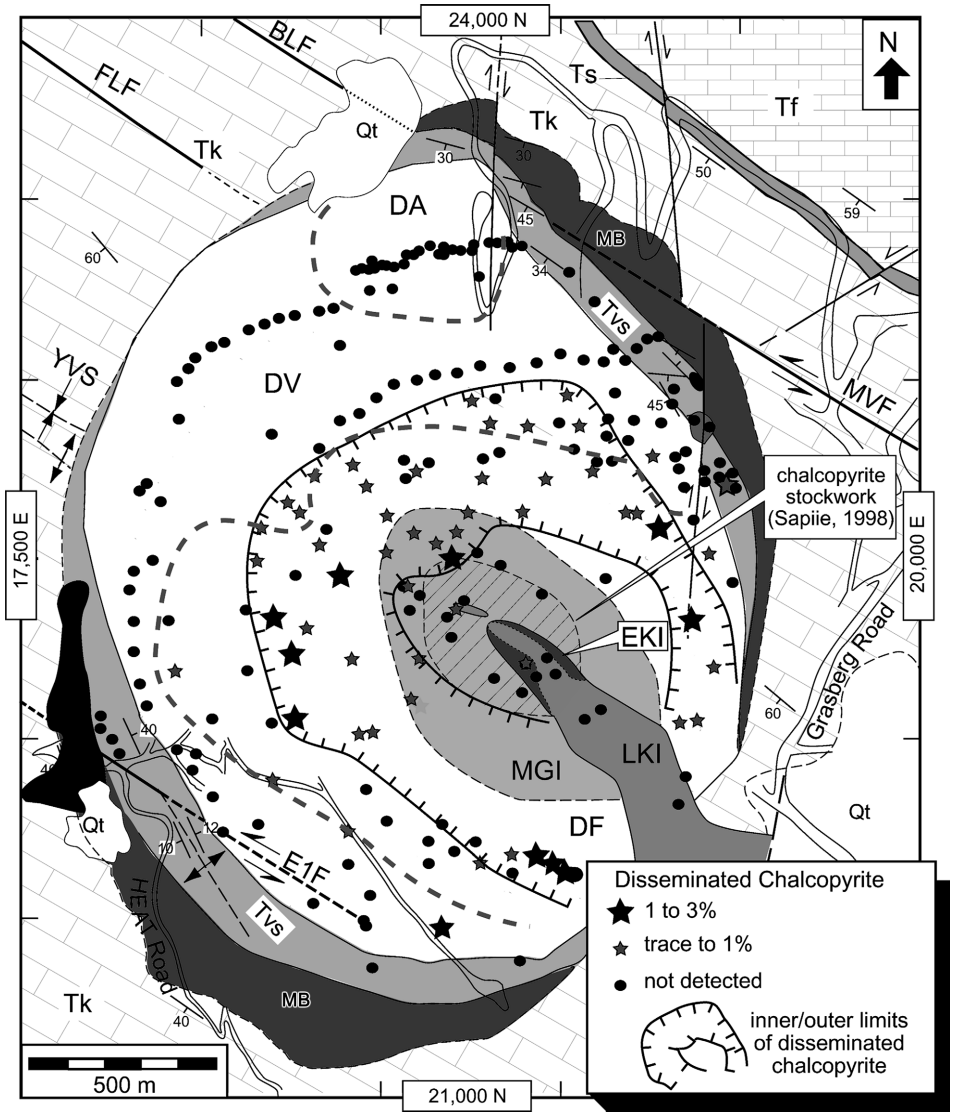

Figure 12: ***Distribution and abundance of disseminated chalcopyrite.*** Note the chalcopyrite stockwork zone mapped by Sapiie (1998) is denoted by hatched pattern. Disseminated chalcopyrite is sparse or lacking in most samples from the interior of the deposit where abundant chalcopyrite veining makes the rock high-grade ore

Holland and Malinin (1979) concluded that the reaction typically begins at about 600°C and is complete at temperatures of around 400°C. This oxidation/reduction reaction so profoundly changes the chemical behaviour of cooling magmatic fluids that it can cause the precipitation of coexisting sulphide (pyrite, chalcopyrite, bornite) and sulphate (anhydrite) minerals (Burnham and Ohmoto, 1980; Wood, 1998). The solubility of sulphide minerals is very small and cooling brines containing metal chloride complexes will react to precipitate sulphide minerals as fast as the reaction proceeds (Barnes, 1979). This, in turn drives the build-up of H_2SO_4 and the precipitation of anhydrite once saturation concentrations are attained.

The precipitation of anhydrite from solution is dependent upon the concentration of Ca as well as on the activity of sulphate in solution. As evident from pseudomorphic reactions, the Ca content of the outwards flowing fluids increases because Ca is released by the alteration of plagioclase phenocrysts to biotite (reaction 1) in the core of the GIC and to sericite (reaction 4) towards the periphery. Anhydrite is precipitated from solution via the following reaction:

$$CaCl_2 + H_2SO_4 \rightarrow CaSO_4 + 2HCl \qquad (13)$$

Along the margins of the GIC, anhydrite and sericite replace plagioclase by the reaction:

$$3\ CaAl_2Si_2O_8 + 3H_2SO_4 + 2\ KCl \rightarrow 2KAl_3Si_3O_{10}(OH)_2 + 3CaSO_4 + 2HCl \qquad (14)$$

Blount and Dickson (1969) discovered that anhydrite exhibits the phenomenon of retrograde solubility over a wide range of salinities (Fig. 15). The solubility of anhydrite is a minimum at approximately 300°C and increases sharply with decreasing temperature (see also Moller, 1988; He and Morse, 1993). Thus, hydrothermal fluids cooling from temperatures higher than the solubility minimum (fluids moving outwards through the deposit) will precipitate anhydrite upon cooling until the temperature of the solubility minimum. From that point onwards, fluids can continue to move outwards and/or upwards without precipitating anhydrite. For rocks containing anhydrite, the flow of cooler fluid, or later influx of meteoric waters, will cause dissolution forming porosity.

Thus, first attaining saturation and retrograde solubility are first-order physical explanations for the distribution and abundance of anhydrite in the GIC. Furthermore, this discussion underscores that precipitation of hydrothermal minerals can be attributed to spatial changes in the physical conditions (in this case, primarily temperature), rather than a series of alteration events invoking pulses of different fluid composition in different parts of the deposit.

XRD Analysis of Powdered Samples

Copper porphyry systems typically have an abundance of minerals with a very fine (<30 microns in this study) grain size (Creasey, 1966) and the GIC is no exception (Fig. 16). Clay-sized minerals are abundant towards the periphery of the deposit and only minor components of the interior. Thirty-eight samples distributed around the deposit and representing all units were chosen for analysis of bulk rock powders by x-ray diffraction analysis (XRD). Clay mineral identifications are based upon criteria in Thorez (1976). Analytical techniques are discussed in Paterson (2004).

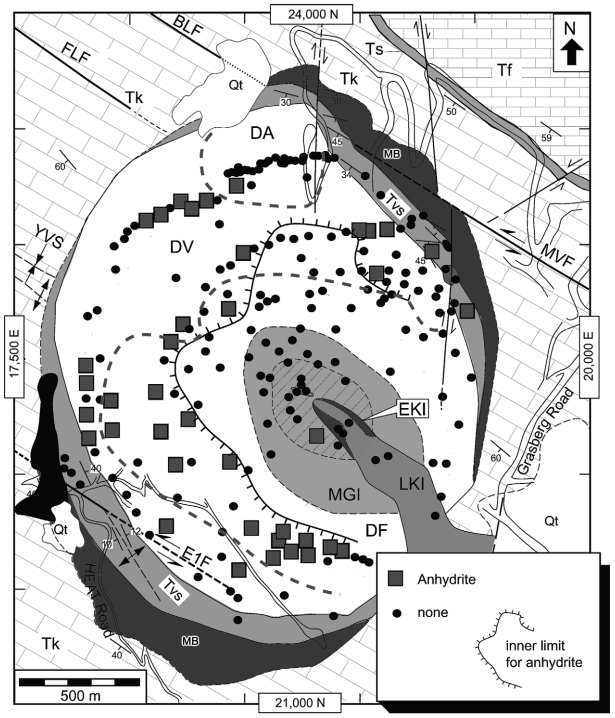

Figure 13: ***Distribution of anhydrite.*** Anhydrite is lacking in the interior of the Grasberg Igneous Complex because it was never present and has been removed from many samples in the exterior as evident from vuggy porosity.

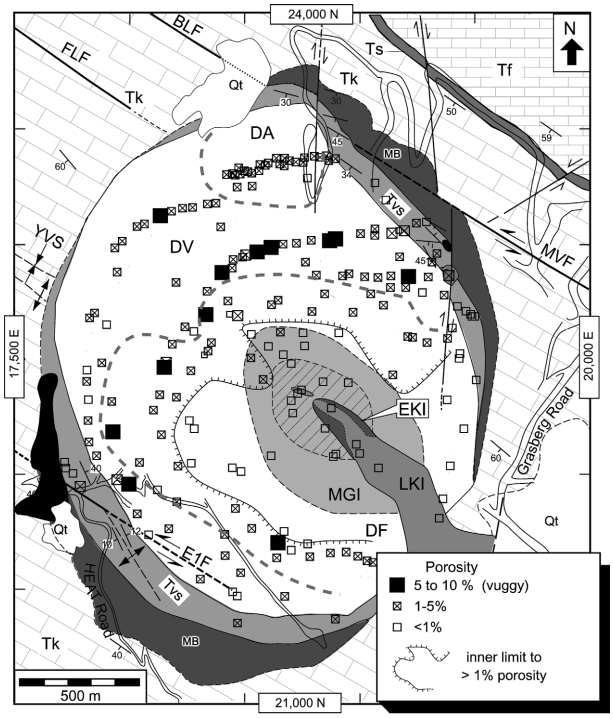

Figure 14: ***Porosity variability.*** Most of the porosity is probably due to the dissolution of anhydrite. Note the low porosities in the centre and the band of high porosities for samples located about 500 m from the centre of the Grasberg Igneous Complex.

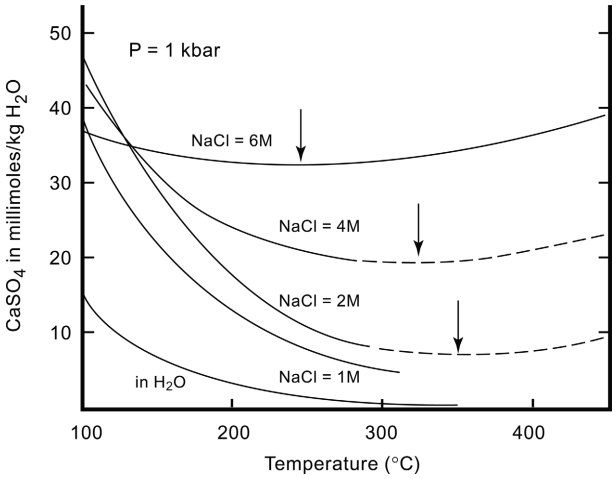

Figure 15: ***Solubility of anhydrite in saline fluids.*** Note the solubility minimum at about 300° C. From Blount and Dickson (1969).

Fig. 17 shows the location of samples and the clay-sized minerals systematically searched for with XRD. Except for some samples containing epidote, sericite is present in all samples located more than about 500 m from the centre of the GIC. As illite is a mica-like clay mineral that is similar to muscovite/sericite but having less potassium and more water, it is not surprising that illite was detected in almost all XRD patterns.

Most importantly, smectite was not detected in the XRD patterns, indicating that, if present, it occurs in quantities below approximately 5%. This is significant because smectite typifies the argillic zone of copper porphyry systems (Hemley and Jones, 1964; Beane and Titley, 1981; Beane, 1982). Smectite is not entirely absent, however. Sapiie (1998) found that clay dykes which extend into the deposit contain abundant smectite. Using techniques to concentrate clay-sized mineral fractions, Penniston-Dorland (1997) detected small amounts of smectite in alteration halos around pyrite veins. It is clear that smectite is not a significant product of pervasive hydrothermal fluid alteration in the open pit samples included in this study.

Illite, chlorite, and kaolinite were not detected in the samples from the interior of the GIC. Chlorite was detected in nine samples, mostly in the southwest part of the GIC. Swelling chlorite was detected in two samples from near the northeast margin. Kaolinite was detected in 14 samples and is most abundant near the margins of the deposit. Most samples that contain kaolinite also contain illite (11 of 15 samples), but only about half of the samples that contain illite also contain kaolinite (11 of 23 samples).

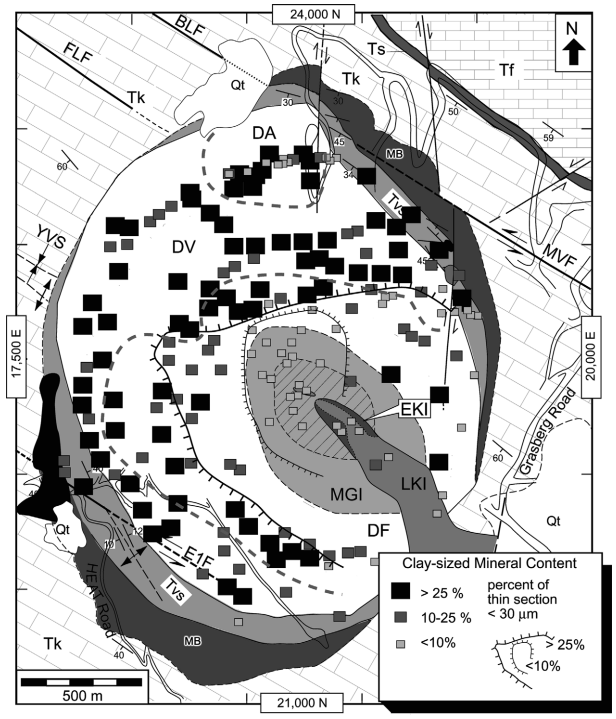

Figure 16: ***Distribution and abundance of clay-sized minerals.*** This is a visual estimate of the percentage of a thin section occupied by minerals <30 microns across.

Overprinting Hydrothermal Replacements

Direct evidence for the thermal and chemical evolution of the GIC comes from the observation of hydrothermal minerals that are themselves replaced by other hydrothermal minerals. The most common is sericite replacement of biotite. Another distinctive relationship is chlorite replacement of biotite. Pyrite is found to overgrow or replace magnetite in many samples.

Sericite Replacing Hydrothermal Biotite

The petrographic observation of sericite replacing hydrothermal biotite is distinctive but volumetrically minor with replacement of never more than about 1% by volume

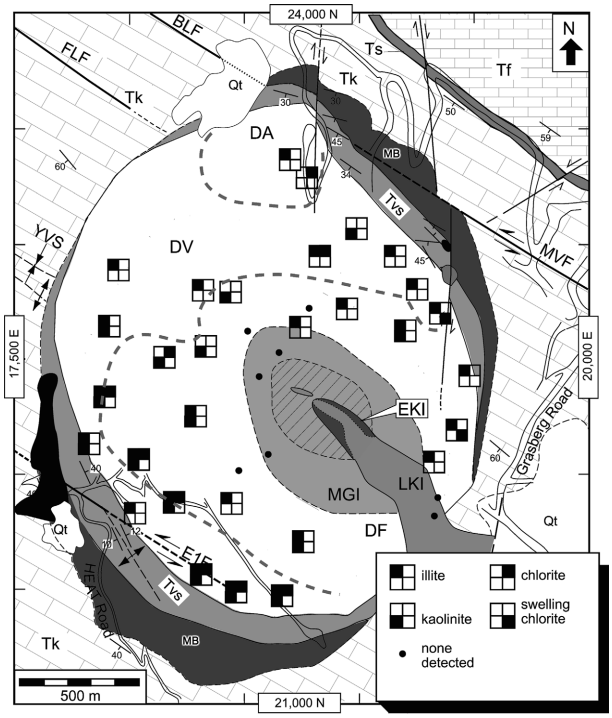

Figure 17: ***Diagram showing samples selected for x-ray diffraction analysis of bulk powders to detect the presence of illite, kaolinite, smectite, and chlorite.*** Note that the samples from the interior lack these minerals. Swelling chlorite was detected in two samples. Smectite was not detected in any sample, but is probably present in trace amounts.

of the biotite present. The spatial distribution of sericite replacing biotite (Fig. 18) defines an annular region about 500 m wide that surrounds the core of the deposit. A critical observation is that sericite always replaces hydrothermal biotite and never the opposite. The idealised replacement reaction is:

$$3KFM_3Si_3AlO_{10}(OH)_2 + 20HCl \rightarrow KAl_2Si_3AlO_{10}(OH)_2 + 9FMCl_2 + 2KCl + 6SiO_2 + 12H_2O \quad (15)$$

This is an acid-consuming, metal-releasing reaction.

Chlorite Replacing Biotite

Chlorite (commonly with trace amounts of pyrite) is widely distributed as thin coatings on joint surfaces in most of the GIC (Sapiie, 1988). However, chlorite identifiable in thin section is absent from most of the deposit. Thin rims of chlorite mantle hydrothermal biotite in a zone about 500 x 800 m zone centred about 250 m northwest of the centre of the deposit (Fig. 19).

In these rocks, chlorite is coarse enough to identify petrographically, but too low in abundance to be detected with x-ray diffraction methods. Much like the replacement of hydrothermal biotite by sericite, this alteration never replaces more than about 1% of the volume of biotite. Only the replacement of hydrothermal biotite by chlorite is observed, not the opposite. The idealised chemistry of this replacement is:

$$2KFM_3Si_3AlO_{10}(OH)_2 + 4HCl \rightarrow FM_5AlSi_3AlO_{10}(OH)_8 + 3SiO_2 + FMCl_2 + 2KCl \quad (16)$$

The replacement of biotite by chlorite in the interior and sericite in the exterior are both late-stage, acid-consuming, metal-releasing reactions that are unidirectional in their occurrence. They are both manifestations of the final stage of pervasive fluid flow when the hydrothermal system was cooling.

Pyrite and Magnetite

Pyrite rims, intergrowths, or replacements of magnetite are readily apparent in many thin sections from a horseshoe-shaped region about 200 to 400 m wide, centred about 500 m from the centre of the GIC (Fig. 20). There are scattered occurrences of this phenomenon in samples of the Dalam.

As magnetite occurs in irregular masses, there is no obvious distinction between overgrowths (with a discontinuous growth history), intergrowths (co-existing growth), and replacement by pyrite. However, as sericite is found replacing biotite in most of the same thin sections, it seems certain that some, if not most, of these masses are pyrite replacements of magnetite.

An idealised chemistry for the replacement of magnetite by pyrite is:

$$3Fe_3O_4 + 16H_2S + 2SO_2 \rightarrow 9FeS_2 + 16H_2O \quad (17)$$

In contrast to the acid-consuming reactions previously identified, this reaction requires a high activity of reduced sulphur to proceed. The abundance of magnetite in the core of the deposit and pyrite in the exterior indicates that hydrogen sulphide only became abundant as the infiltrating fluids moved outwards, consistent with the concept that cooling and hydrolysis of SO_2-rich fluids caused sulphide mineral and anhydrite precipitation.

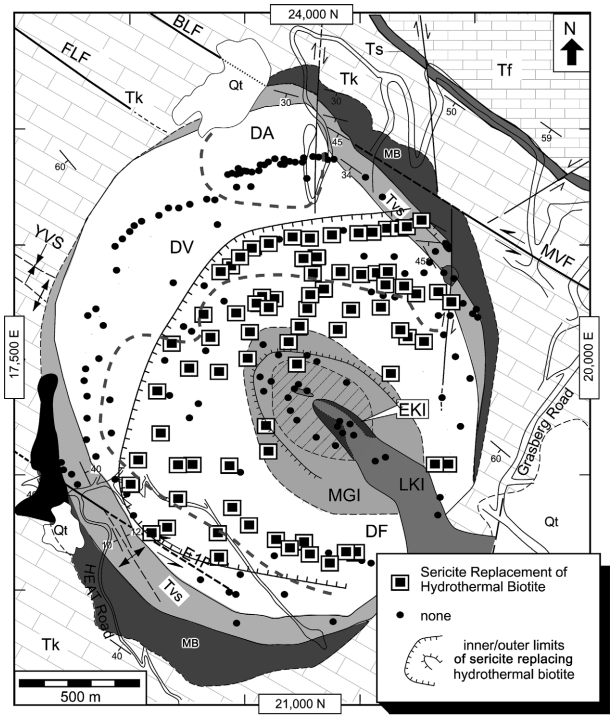

Figure 18: ***Distribution of sericite replacing hydrothermal biotite.*** In most samples in the interior of the deposits, only trace amounts of sericite are present.

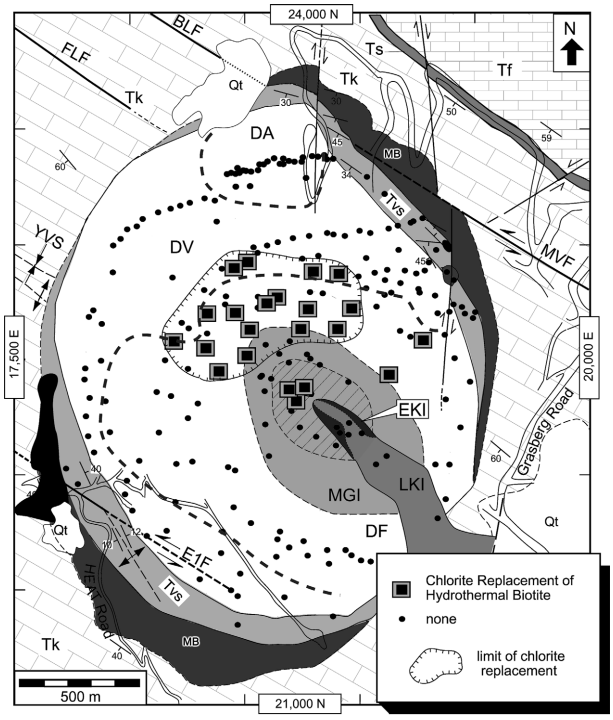

Figure 19: ***Distribution of chlorite replacement of hydrothermal biotite.*** This replacement typically only occurs in trace amounts.

Trace Heavy Metal Phases

Reflected light petrography of 225 samples combined with microprobe x-ray mapping of the groundmass in 18 samples revealed remarkably little evidence for opaque phases other than magnetite, pyrite and chalcopyrite. Enargite, an arsenic-bearing phase was found in one sample (00-MC-37) and a few grains of Zn-bearing sulphide were noted in another (00-MC-03). Heavy-metal-bearing trace phases containing Pb, Zn, As, Hg, etc., are widely noted in other copper porphyry deposits; their scarcity in the GIC requires an explanation and is discussed below.

Alteration Zones

The Grasberg copper-gold orebody displays mineral alteration zoning that is overall very similar to that reported in other copper porphyry systems. In this study, alteration zones in the Grasberg are named in terms of the major mineral assemblages, as is common practice in characterising metamorphic terranes. The lateral mineralogic zonation is summarised in Fig. 21. Fig. 22 is a summary map which shows that the limits to alteration zones form roughly concentric rings within the Dalam and MGI, centred on the core of the GIC.

Biotite + Magnetite Zone ≈ Potassic Alteration

"Potassic" alteration dominates the interior portions of many porphyry copper deposits. In most classifications, the requisite assemblage is potassium feldspar + biotite (Lowell and Guilbert, 1970; Titley, 1982). This mineralogic criteria becomes problematic when applied to potassic magmatic rocks. McMahon (1994a, b, c) placed all of the igneous rocks in the GIC into a high-K suite. Potassium feldspar is abundant in the magmatic groundmass of the Kali (Paterson and Cloos, this volume). Thus the presence of potassium feldspar in the GIC is not, by itself, diagnostic of alteration. The same problem applies to magnetite, which is only confirmed as a magmatic phase in Kali phase intrusions, but probably was present in other units as well. The centre of the GIC hydrothermal system also produced andalusite, a mineral not widely reported in most similar deposits.

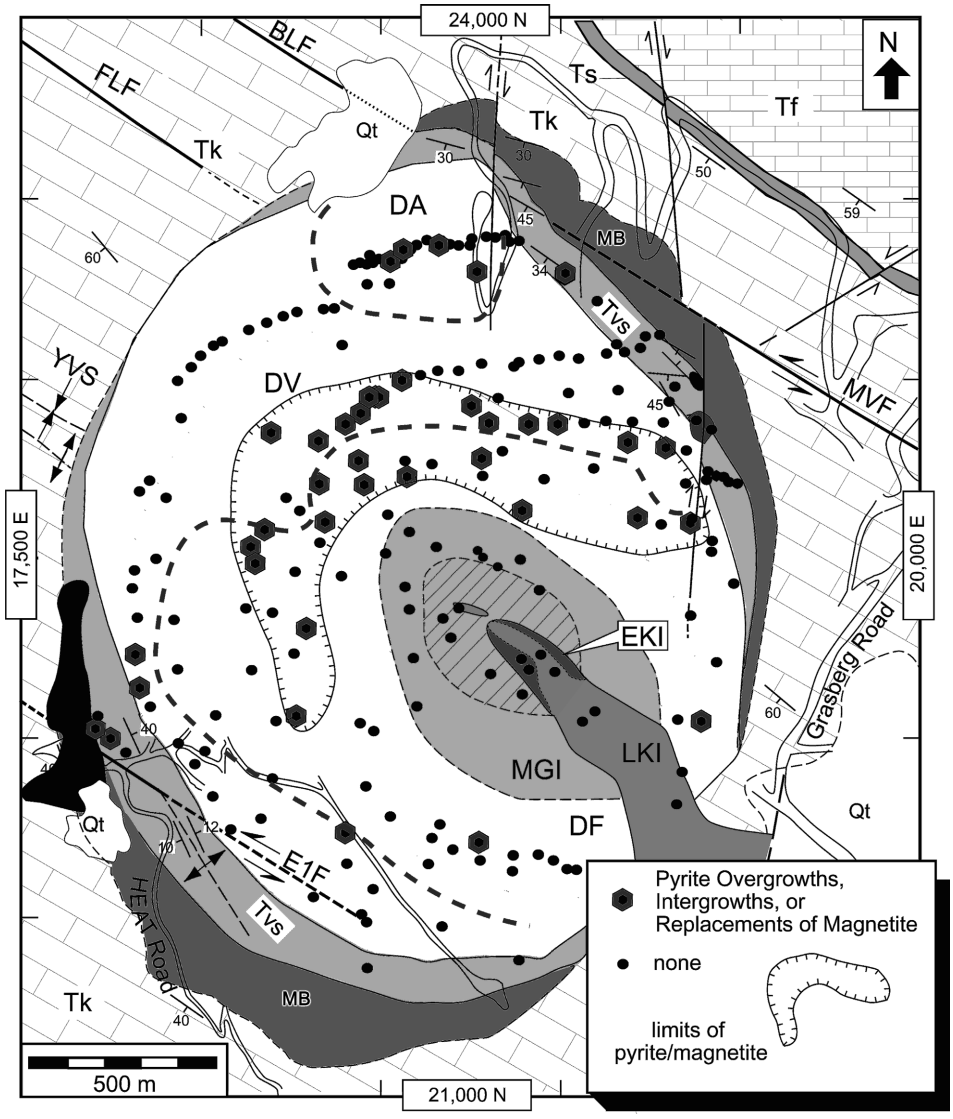

Figure 20: ***Distribution of pyrite overgrowths, intergrowths or replacements of magnetite.*** Where present, pyrite is present on the exterior of the magnetite grains.

Shreddy biotite is the only diagnostic alteration mineral in the high temperature interior of the deposit. Disseminated magnetite is so abundant and intimately intergrown with shreddy biotite that it also must be an alteration product. That fluids precipitated magnetite, is directly evident from the abundant veins of quartz + magnetite in the core of the deposit, and the less common, but widely occurring magnetite-only veins. Outside of the Kali phase intrusions, the association of hydrothermal biotite with magnetite comprises as much as 60% of the innermost Dalam (DF) and MGI. In the GIC, the mineral assemblage biotite + magnetite with an inner sub-zone containing andalusite is the equivalent of the potassic zone. Fluid infiltration and alteration in the core of the GIC was pervasive to the finest scales of observation.

Sericite + Anhydrite + Pyrite Zone ≈ Phyllic Alteration

"Phyllic" alteration comprises large areas in the outer part of many porphyry copper deposits. The requisite assemblage is sericite + quartz + pyrite (Lowell and Guilbert, 1970; Titley, 1982). In the GIC, quartz is not diagnostic of conditions as it is ubiquitous. Moreover, in much of this deposit, it is clear that sericite and pyrite are intimately associated with anhydrite (compare Fig. 13 [anhydrite] and Fig. 14 [porosity] with Fig. 7 [sericite] and Fig. 10 [pyrite]). In the GIC, the mineral assemblage sericite + anhydrite + pyrite is the equivalent of the phyllic zone.

The degree of alteration in the sericite + anhydrite + pyrite zone is variable. About 500 m from the centre of the deposit, it is locally so intense that all evidence of the original igneous mineralogy is destroyed (Fig. 2). This style of alteration is locally weak or absent in the outer part of the GIC indicating fluid infiltration was not as pervasive as in the interior near the fluid source.

Alteration Zone Overlap/Overprint Phyllic

A phyllic overprinting of the potassic zone is reported in almost all copper porphyry deposits (Beane, 1982), while in some, there is a near total overprint of the potassic zone by the phyllic alteration. Examples include the Superior District, Arizona (Manske and Paul, 2002), and Island Copper Porphyry, British Columbia (Arancibia and Clark 1996).

Gustafson and Hunt (1975) proposed that the original alteration assemblage at El Salvador, Chile, graded outwards from potassic directly into propylitic alteration. Only upon the later invasion of meteoric water into the deposit did phyllic alteration overprint the potassic zone. A persistent concept has been the notion that phyllic alteration is the product of the invasion of meteoric water into the system (Taylor, 1974). However, increasing evidence indicates the contrary, that phyllic alteration fluids are magmatically derived (Hedenquist *et al.,* 1998; Richards *et al.,* 1998). Harris and Golding (2002) reported oxygen and hydrogen isotope compositions of vein quartz from the Endeavour 26N Cu-Au porphyry in Australia, and compared their results to published data from El Salvador, Chile, Panguna and Porgera, Papua New Guinea, and Far Southeast, Philippines. They concluded that magmatic fluids caused phyllic-type alteration in all of these deposits.

Fig. 23 shows that there is a 150 to 300 m wide, horseshoe-shaped zone where the sericite + pyrite + anhydrite zone overlaps the biotite + magnetite zone. Some overlap of these zones is expected because the transition from one to the other should not be abrupt because both solid and fluid solutions are involved. Two mapped textural relationships are clear recorders of replacement: i) sericite and pyrite replacing biotite (Fig. 18; reaction 6), and ii) pyrite

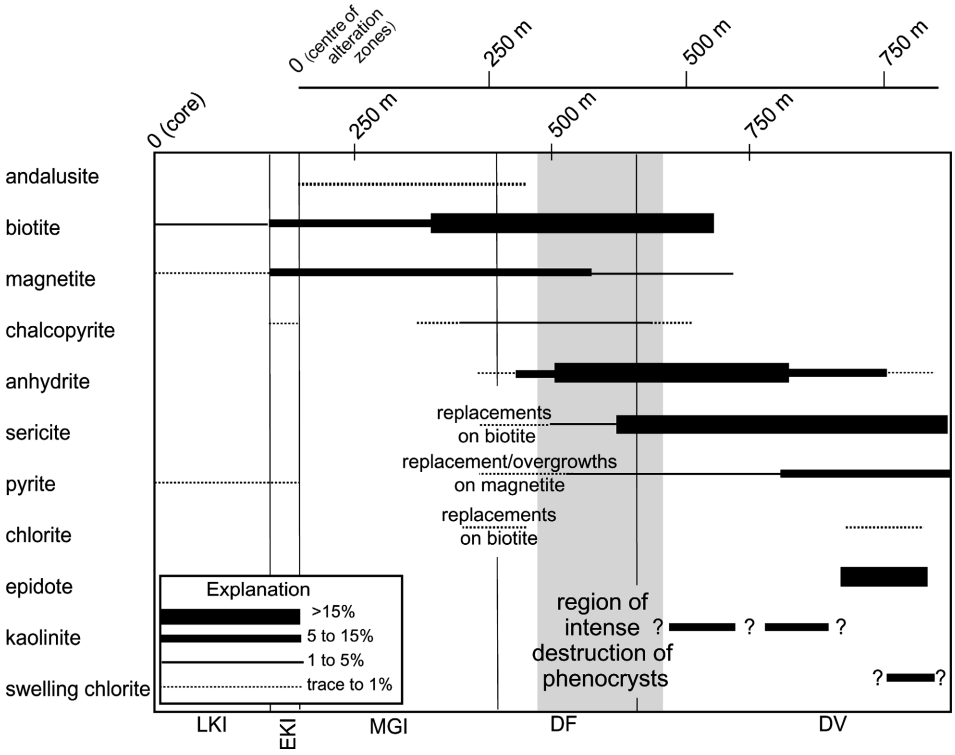

Figure 21: ***Schematic pattern of mineral replacements due to pervasive alteration.***

replacing magnetite (Fig. 20; reaction 17). Samples containing pyrite that is probably replacing magnetite show a similar pattern.

Cooling of chlorine-rich, SO_2-bearing magmatic fluid will cause an increase in the activity of acid and hydrogen sulphide that would drive these replacements. Consequently, cooling of the system because heat advection into it was lessened by the slowing of hydrothermal fluid flow will cause a mineralogic overprint near the boundary between the two zones of alteration. It is notable that no petrographic evidence (biotite + magnetite replacing sericite + anhydrite + pyrite) was found for an increase in temperature and flow rate.

The temperature of the fluid is the primary control on the mineral assemblage that develops, although it is the volume of flow that determines the extent of reaction. The minor extent of alteration overprint in the GIC indicates hydrothermal flow rates must have decreased dramatically once substantial cooling of the system had begun. The simplest explanation for the observed overprinting relationships is that the outflow of magmatic fluids did not slowly wane, but instead ended rather abruptly.

Epidote ± Chlorite Zone ≈ Propylitic Zone

Epidote is confined to the periphery of the GIC where it replaces plagioclase. In the samples that contain(ed) abundant biotite or amphibole, chlorite is abundant. At the deposit scale, epidote ± chlorite alteration occurs in patches forming islands surrounded by sericite + anhydrite + pyrite alteration (Fig. 9). Some thin sections that contain epidote ± chlorite, have sericite and pyrite in the groundmass. However, no direct evidence of the replacement of epidote ± chlorite by the sericite and pyrite assemblage was found.

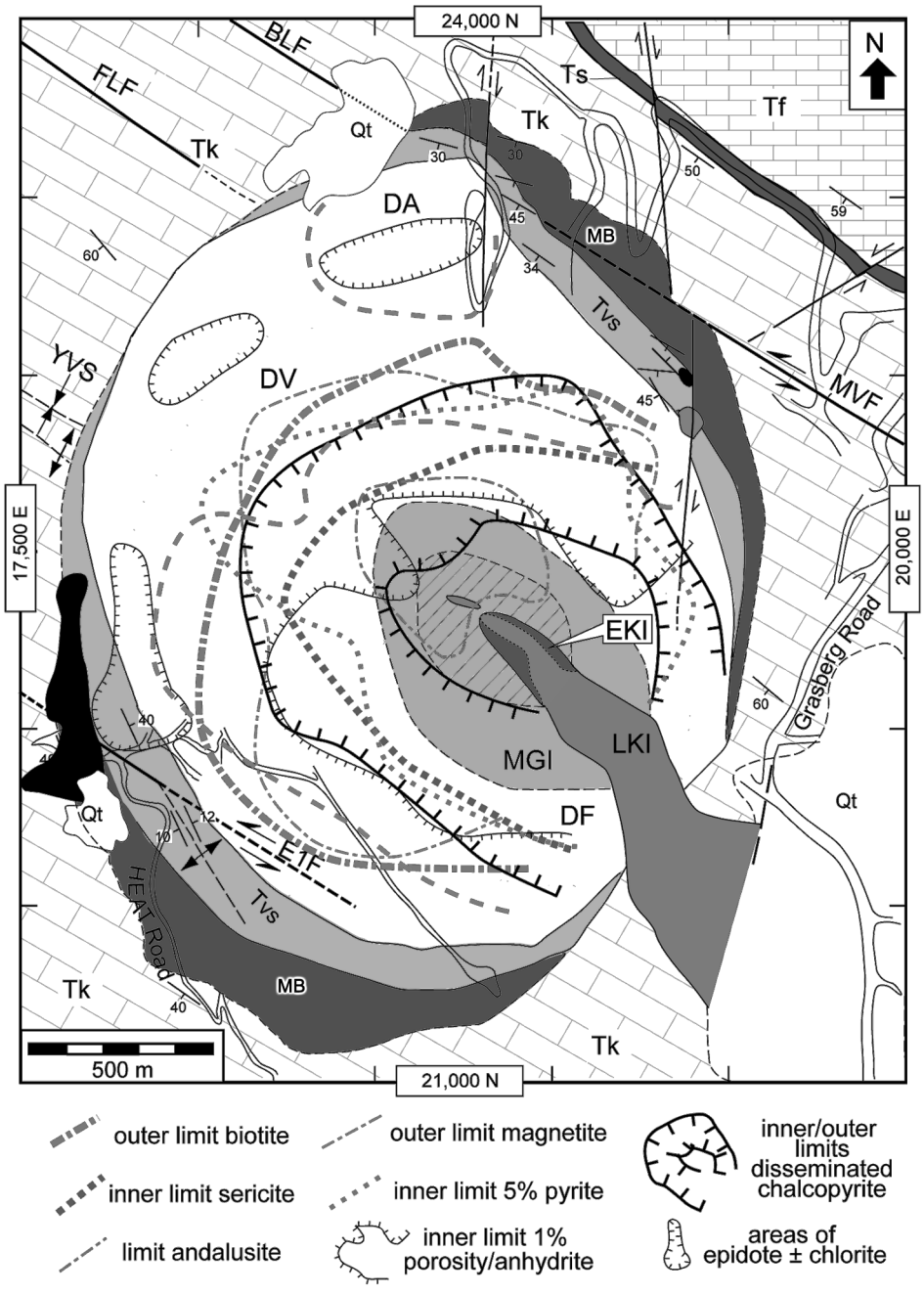

Figure 22: ***Spatial limits of pervasive alteration zones.***

Epidote, chlorite and albite are products of near-isochemical metamorphism under greenschist facies conditions (~300°C) (Beane, 1982; Berger and Velde, 1992). The islands of epidote ± chlorite along the edges of the GIC are regions where the igneous rock was kept at elevated temperatures for a prolonged period without the invasion of acidic hydrothermal fluids. This indicates the hydrothermal flow causing alteration was less pervasive along the edges of the deposit.

Kaolinite Occurrence ≈ Argillic Alteration

The simplest criteria for argillic alteration is the presence of abundant clay minerals, commonly smectite or kaolinite (Creasey, 1966). Advanced argillic alteration (higher temperature) is characterised as abundant quartz in association with kaolinite, pyrophyllite and alunite (Reed, 1997). The formation of clays from feldspars involves the leaching of alkalis at low (<200°C) temperatures. In some deposits, the mapping of the extent of argillic alteration has proven problematic. Recently, Williams and Forrester (1995, p. 26) stated that "the so-called argillic zone is virtually a myth because detailed work on clays from 'magmatic argillic zones' invariably demonstrates the clay to be sericite."

The XRD analyses in this investigation of bulk rock powders revealed small amounts of kaolinite in many samples. Most notably, smectite was not detected in any of the bulk powders. Penniston-Dorland (1997) performed clay-size separations and analysed the clay fraction of several samples, finding kaolinite along with trace amounts of smectite in the alteration halos that border some of the pyrite ± quartz veins. Sapiie (1998) reported that smectite is the major component of clay dykes that were a volumetrically minor, but common, feature in the Grasberg open pit prior to 1996 (locations higher than about 3700 m elevation). If the presence of smectite is considered essential to document argillic alteration, the GIC has no systematically developed argillic zone.

Using the presence of kaolinite as the criterion, "argillic" alteration is widely developed in the GIC, but of trivial volume. Kaolinite should form from feldspars wherever cool (<200°C), acidic fluid is present. Hence, the minor development of kaolinite is another indicator that cooling

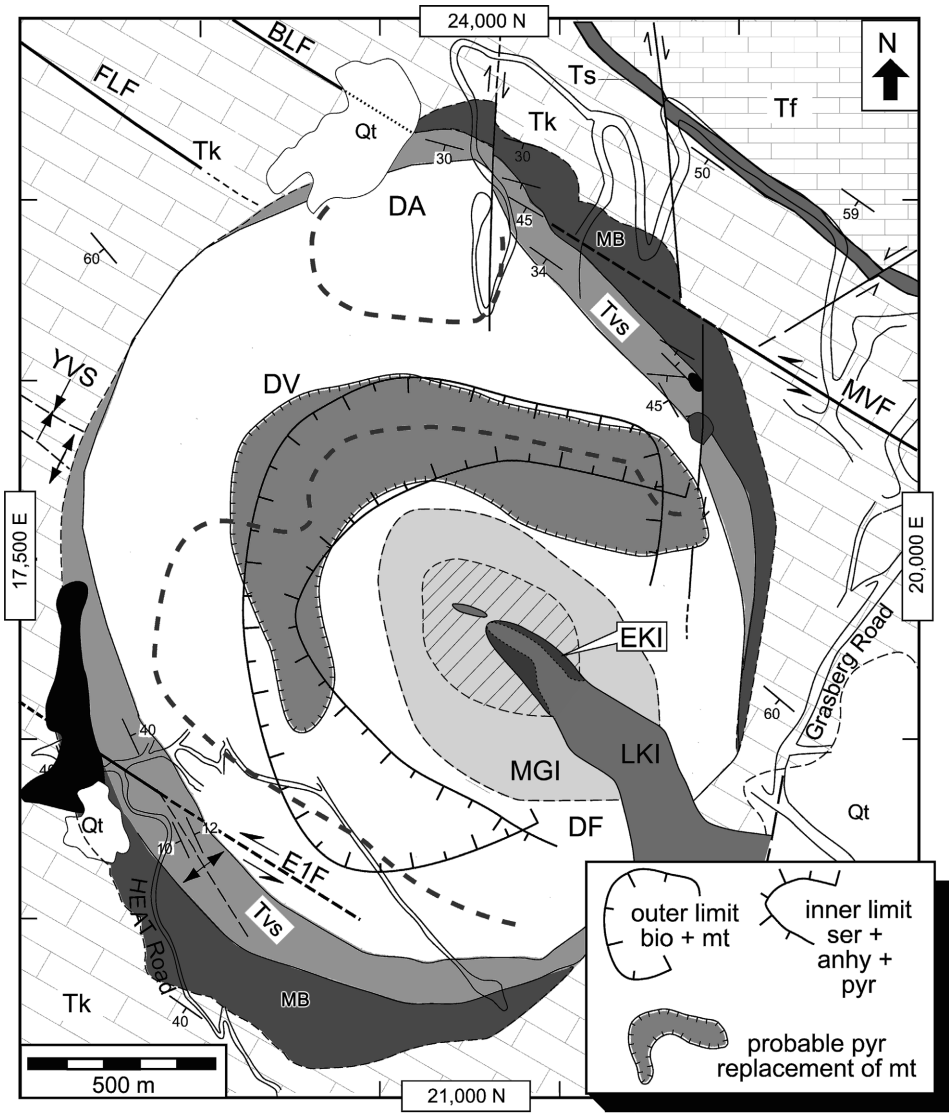

Figure 23: ***Region where sericite + anhydrite + pyrite alteration overlaps biotite + magnetite alteration.*** Area where pyrite overlaps magnetite is shaded. Note the horseshoe-shaped regions of mineralogic overlap at the ~3900 m elevation of the open pit mine.

of the deposit to ambient thermal gradients was not concurrent with the flow of substantial volumes of hydrothermal fluid.

Scarcity of Heavy Metal Phases

Grasberg ore has very low contents of elements such as Pb, Zn, As and Hg (MacDonald and Arnold, 1994). There are two explanations for their scarcity: i) the initial concentration of these species in the mineralising fluids was lower than other systems, and/or, ii) final cooling of the system to ambient thermal gradients was not concurrent with substantial fluid flow.

The solubilities of Pb, Zn, As, Hg and many other trace metals increase exponentially with increasing temperature (Barnes, 1979; Wood and Samson, 1998). For common abundances in magmatic fluids, these metals typically do not form phases at temperatures of 300°C or higher. Sphalerite and galena are present in scattered veins and pods outside the Grasberg. Several examples outcrop along the HEAT road (Sapiie, 1998). Small amounts of sphalerite and galena are present along the outer edges of the cylindrical body of massive pyrite (the "Heavy Sulphide Zone") at the 3045 m elevation of the Kucing Liar and Amole Drifts (Lambert, 2000). Larger pods are present at the surface in the marginal breccias (Fig. 2, northeast corner of the GIC, Sapiie, 1998). The deposition of Pb and Zn at these locations is not surprising, as the fluids reaching the edges of the deposit would have been at temperatures much less than 300°C. The key observation is that Grasberg system fluids did contain Pb and Zn in sufficient quantities to form scattered deposits of base metals.

More diagnostically, Ulrich *et al.,* (1999) analysed a few fluid inclusions from a Grasberg sample and found that their concentrations of zinc and lead significantly exceeded that found in the bulk ore. From this observation and their detailed study of inclusions from the Bajo de La Alumbrera deposit (see Ulrich and Heinrich, 2001), they concluded that: "very large quantities of ore metals are flushed through ore deposits, and ultimately become dispersed unless steep thermal and chemical gradients provide a driving force for efficient mineral precipitation" (p. 678).

The trace-metal contents of Grasberg system fluids may have been lower than other systems, but there is no reason to believe these fluids had exceptionally low trace-metal contents compared to other deposits. The conclusion is that Zn, Pb, As, Hg and other trace metals flushed through the system as large volumes of Cu and Au were precipitating. The scarcity of trace metals is yet another indicator that cooling of the deposit to ambient thermal gradients was not concurrent with the flow of substantial volumes of hydrothermal fluid.

Discussion

Petrography combined with x-ray diffraction analysis shows that the pervasive fluid flow that affected the Dalam and MGI phases of intrusion at the ~3900 m elevation generated mineral assemblages that define several roughly circular alteration zones (Fig. 22). The Late Kali phase postdates essentially all pervasive fluid flow, whereas the Early Kali phase, which is veined and locally altered, but much less so than the MGI, postdates all but the final stage of pervasive fluid flow.

Biotite + magnetite alteration, with an inner sub-zone containing andalusite affected the MGI and the innermost Dalam whereas sericite + anhydrite + pyrite alteration dominates alteration in the exterior of the deposit. The widespread, but minor occurrence of kaolinite and the local replacement of biotite by chlorite are products of the cooling of the Grasberg system to ambient thermal gradients. The "islands" of epidote ± chlorite near the edges of the GIC delineate areas where thermal metamorphism occurred, but thoroughly pervasive fluid infiltration did not. The chemistry of the hydrothermal mineral-forming reactions can be divided into two groups: i) an inner zone dominated by biotite + magnetite that is hot and acid generating, and ii) an outer zone of sericite + anhydrite + pyrite that is cooler and acid-consuming.

Acid Production and Consumption – The Chemistry of Fluid Flow

Intense acid attack is a long-known and widely described characteristic of hydrothermal alteration in the phyllic zone of copper porphyry systems (Guilbert and Park, 1985). Beane and Bodnar (1995) conclude that fluids in all copper systems increase in acidity as they move from the potassic to phyllic to argillic zones. Acid production in the inner part and consumption in the outer part explains the overall pattern of alteration in the GIC as well.

Significant acid production in the core of the deposit would have resulted from the high-temperature precipitation of abundant magnetite (reaction 10). At slightly lower temperatures, the precipitation of chalcopyrite (reaction 11) added to the acidity of the fluid. Associated silicate alteration reactions, producing hydrothermal biotite in the interior of the deposit, were also acid-producing (reactions 1, 2, and 3). It is most likely that the magmatic fluids altering the core of the GIC only become acidic (by forming HCl which dissociates into H^+ and Cl^- complexes) after magnetite precipitation begins.

Temperature variations in the Grasberg hydrothermal system are broadly constrained. The fluids are magmatic and would have been exsolved at temperatures of 800 to 1000°C. The best direct petrologic indicator of the highest temperature conditions during pervasive infiltration comes from the presence of andalusite in a zone approximately 500 m across centred on the core of the deposit (Fig. 9). Andalusite, however only indicates temperatures were greater than 425°C (Paterson, 2004). Fluid-inclusion homogenisation temperatures for quartz from the stockwork zone indicate temperatures in the centre of the GIC were actually much hotter, 600°C and higher (Harrison 1999). Maximum temperatures in the marginal breccias that outcrop at the surface were mostly less than 200°C (Sapiie, 1998). Halloysite, which has an upper thermal stability of 110°C, is present in the banded clay unit that outcrops on the southwest and northeast edges of the deposit.

Magmatic fluids can incorporate large amounts of sulphur as SO_2. The precipitation of sulphide minerals and anhydrite can only begin after SO_2 in the fluid begins to

hydrolyse (reaction 12). As discussed in the section on anhydrite, the production of H_2S and H_2SO_4 occurs across the temperature range from about 600 to 400°C (Holland and Malinin, 1979). The local concentration of sulphide and sulphate species in the fluid reflects the primary SO_2 content, the thermal gradient along the flow path, and the solubilities of sulphide and sulphate mineral species.

The scarcity of disseminated sulphide minerals in the core of the GIC, where biotite + magnetite alteration is extensive, is explainable as the infiltrating fluids were too hot to hydrolyse SO_2. Upon cooling to about 600°C, the first reduced sulphur is generated. Chalcopyrite precipitation begins and continues until the fluids became depleted in copper at temperatures of about 400°C. Pyrite precipitation begins where temperatures have cooled to about 450°C. Pyrite mineralisation continues to the edge of the deposit, in part because iron is steadily released by the replacement of mafic phases by sericite (reaction 6). Reduced sulphur would have been steadily removed from the fluid by the growth and precipitation of chalcopyrite and pyrite. In contrast, the sulphate content of the fluid would have steadily increased until the point where anhydrite precipitation begins (Fig. 25).

The replacement of plagioclase by biotite (reaction 1) and sericite (reaction 5) liberates Ca to the fluids (reaction 1). Consequently, the calcium ion content in the migrating fluids must have steadily increased as the fluids migrated outwards. Disseminated anhydrite is essentially absent in the core of the open pit mine (Figs. 13 and 14) and it is thus evident that anhydrite saturation did not occur until the temperatures decreased to about 450°C. Once this occurred, the alteration assemblage became sericite + anhydrite + pyrite. Where temperatures were less than about 300°C, retrograde solubility prevented further precipitation of anhydrite.

The chemical evolution of the fluids migrating outwards form the core of the system can be summarised as a sequence of zones (Fig. 24). Zone A (not exposed) is primary, near-neutral magmatic fluid at 800°C or so that is little modified by interaction with cooler rock. Zone B is where magnetite precipitation occurs, thereby beginning the increase in the acidity of the fluid. Temperatures were probably about 700 °C when magnetite precipitation begins. Zone C begins where temperatures of about 600°C were attained, and the hydrolysis of SO_2 produces H_2SO_4 and H_2S. While the concentration of H_2SO_4 increases with further cooling, the concentration of H_2S remains low because chalcopyrite (bornite at depth) and then pyrite precipitate about as fast as H_2S is produced in solution. The precipitation of abundant pyrite generates substantial HCl that along with the build-up of H_2SO_4 causes attack of the wall rock. Zone D, beginning at temperatures of about 450°C, is where H_2SO_4 reacts with $CaCl_2$ (abundant Ca was released from the replacement of plagioclase) to precipitate anhydrite. Acid attack of the host rock, locally so strong that all magmatic textures are destroyed, was strongest in the inner part of zone D. Zone E, at temperatures of about 300°C, is where anhydrite precipitation lessens because of the retrograde solubility of anhydrite. From this point to the edge of the GIC, the concentration of H_2SO_4 in the fluid increases. Alteration is more heterogeneous in the other part of the GIC because the fluid pressure gradients driving the flow are small. When the highly acidic fluids reached the edges of the GIC, they were neutralised by dissolution of carbonate wall rock which formed the extensive zone of marginal breccias (Figs. 2 and 3).

Continuity of Alteration and Copper Mineralisation

MacDonald and Arnold (1994) previously stated that pervasive hydrothermal alteration in the Dalam was the most laterally and vertically extensive. As they believed the MGI was less altered, they concluded that substantial alteration predated the MGI. This study concludes that there is a continuity of pervasive alteration from the MGI to Dalam phase rocks. Alteration in the MGI appears less intense because the host rocks were still very hot when infiltrated by near-neutral fluids at near-magmatic temperatures. In other words, most of the fluids infiltrating the MGI were nearly in equilibrium with the igneous rock.

The apparently greater intensity of Dalam alteration versus the MGI is primarily due to increased acidity and lower temperatures of the fluids as they moved outwards. Another likely factor is that Dalam phase rocks probably had a

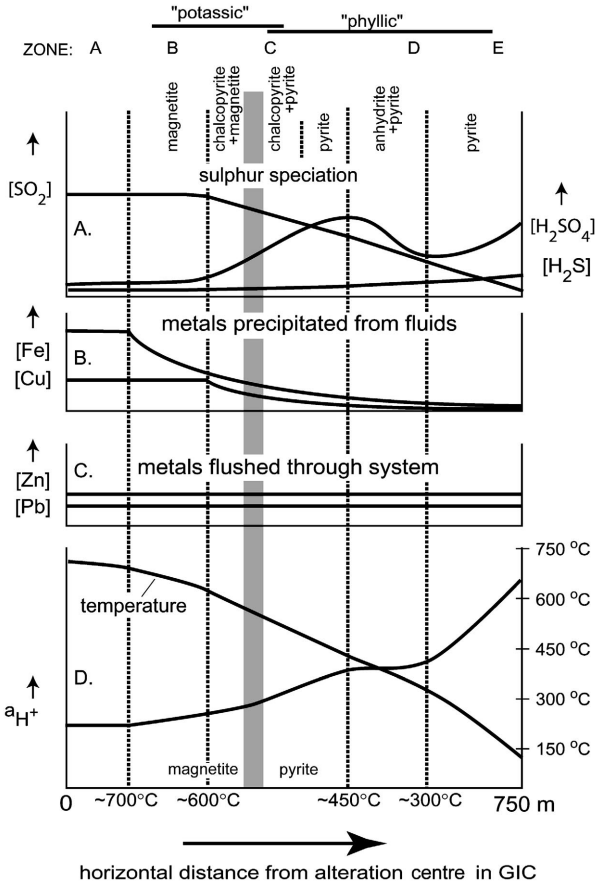

Figure 24: ***Interpreted evolution of chemistry of fluids causing pervasive alteration.***

A. Sulphur speciation.

B. Fe and Cu concentrations.

C. Zn and Pb concentrations.

D. Temperature and acidity **(a^{H+}).**

glassy, highly reactive groundmass. The MGI, which solidified more slowly, was fully crystalline and thus somewhat less reactive.

Most of the copper mineralisation in the Dalam is disseminated while that in the MGI is in veins. Much of the high-grade MGI ore in the core of the deposit contains a stockwork of chalcopyrite veins that are millimetres to centimetres across (limits identified on Fig. 2). This difference in the dominant style of copper mineralisation was interpreted by MacDonald and Arnold (1994) to indicate two distinct phases of mineralisation. Instead, we believe the difference is explainable by differences in the chemical behaviour of fluids flowing in fractures versus those infiltrating the rock. Precipitation of minerals in veins is primarily controlled by fluid chemistry and solubility relationships (fluid-buffered reactions). Growth of disseminated minerals because of pervasive fluid infiltration is primarily controlled by the chemistry of the host rock and the fluid which had exchanged with rock it has previously flowed through (rock-buffered reactions).

No petrographic evidence was detected for a pervasive alteration event that only affected the Dalam phase rocks, but admittedly, the alteration and copper mineralisation event that affected the MGI and Dalam is so intense that an earlier mild event may have been obliterated.

Interpreted History of Intrusion and Mineralisation

The interpreted history of intrusion, pervasive hydrothermal alteration and mineralisation in the Grasberg is as follows. i) Emplacement of the Dalam phase rocks. ii) Intrusion of MGI as a plug into the still-hot core of the Dalam. iii) Intense fracturing in the MGI core of the system, first forming a stockwork of quartz + magnetite veins (Stage 1a), and then chalcopyrite veins (Stage 1b). This stockwork-forming event in the core of the system was concurrent with the massive outflow of fluid that caused disseminated copper mineralisation. Pervasive infiltration formed a concentric mineralogic zonation in which andalusite + biotite + magnetite and then biotite + magnetite was surrounded by sericite + anhydrite + pyrite. Islands of epidote ± chlorite are the result of isochemical thermal metamorphism and indicate fluid flow was not thoroughly pervasive in the outermost parts of the GIC. iv) Emplacement of the Kali phase intrusions. The LKI postdates essentially all pervasive alteration and most veining. The EKI was intruded very near the end of alteration/mineralisation. Stage 2 veining is a comparatively minor event that began after Kali phase intrusion. These fluids were Cu-poor, but also so Al-rich that many veins of biotite were formed.

Final Cooling Without Substantial Fluid Flow

The overprint of the cooler sericite + anhydrite + pyrite zone on the hotter biotite + magnetite zone is of limited width and of very minor intensity. This observation, along with the trivial generation of sericite near the core of the deposit and kaolinite across the deposit, as well as the scarcity of trace metal phases, all indicate the fluid flow system forming the Grasberg did not slowly wane, but rather shutdown abruptly. Cooling of the core of the Grasberg system to temperatures of less than 300°C or so, was not concurrent with significant fluid flow.

It appears that the system cooled to near ambient before emplacement of the Kali phase intrusion, but this is uncertain. Ongoing studies on samples of Kali phase intrusions from the Amole Drift level should enable better understanding of how the EKI relates to alteration and mineralisation.

Centre and Size of the Fluid Source

The centre of the pervasive flow system was near the tip of the wedge-shaped Kali intrusion. Pervasive alteration to biotite + magnetite affected an area about 1200 m across. The inner sub-zone containing andalusite is about 500 m across. Intense quartz/magnetite stockwork veining (Stage 1a) and superimposed chalcopyrite veining (Stage 1b) define a slightly smaller area. As discharging fluid would disperse outward, 500 m is a maximum width for the source of the fluid feeding the system.

Notably, the centre of the alteration as defined by andalusite (Fig. 8), abundant clay-sized minerals (Fig. 16), and chlorite replacing biotite (Fig. 19), are located about 250 m to the northwest. It thus appears that the centre of hydrothermal alteration migrated slightly northwest over time, but this may be an illusion based upon sample distribution.

Reconstruction of the Mineralising System

The fact is, pervasive alteration and veining in the GIC delineates a series of rings that indicates rock-altering fluids emanated from a small source area. Consistent with the picture of Cloos and Sapiie (in review) and Sapiie and Cloos (in press) and the magmatic history deduced in this study (Paterson and Cloos, this volume), the underlying fluid source was the apex of a cupola at the top of an intrusive stock (Fig. 25). If the stockwork veining delineates regions where the roof episodically collapsed over a fluid-charged cupola, a width of 200 to 300 m is indicated. The ceiling of the cupola probably first became fluid charged at an elevation of about 3200 to 3400 m, at a depth below the surface of less than 1000 m. As the system cooled, the cupola would have migrated downwards over time. The pervasive fluid infiltration that formed the concentric alteration zones was driven outwards by a difference in fluid pressure from lithostatic near the cupola to hydrostatic near the surface. Pervasive fluid flow was continuous in space and time and caused steady draining of the cupola that was continuously recharged from below (Cloos, 2001). Superimposed on this "background" flow, causing pervasive alteration, were tectonically-induced extension fracturing events that episodically drained much, if not all, of the accumulated fluid. Fracturing and the upwards jetting of magmatic fluids formed veins with mineralogies that varied because of changes in fluid pressure, temperature, and fluid composition along the flow path (Cloos and Sapiie, in review).

It is evident that lateral thermal gradients in the Grasberg system were very high, on the order of 500°C/km. The near-surface vertical thermal gradient was probably even greater. Extreme thermal gradients and low confining

pressures were important factors that localised precipitation of copper and gold. Fluids at near magmatic temperatures have been detected discharging at the bottom of lakes filling calderas (Giggenbach, 1992), and it seems likely that a bubbling lake in a maar caldera was once atop the Grasberg system (Fig. 25). The banded clay deposits on the southern and northern edges of the GIC are relicts of a field of boiling mud pots. The preservation of the evidence for the extreme lateral thermal gradients indicates that the flow system was probably only active for several tens of thousands of years.

Conclusions

This study documents that pervasive fluid flow in the Grasberg Igneous Complex generated a hydrothermal mineralogy and pattern similar to that in many copper porphyry systems. New to the study of the GIC are the following observations:

i) Andalusite occurs in a ~500 m wide zone in the centre of the GIC.
ii) The replacement of magmatic minerals by later hydrothermal minerals is recorded by phenocryst replacement relationships, and idealised reaction relationships can be identified for all common replacements.
iii) Anhydrite is almost absent in the core of the deposit, and most abundant in a band about 500 m from the centre. The inner and outer limits to anhydrite occurrence were determined by the hydrolysis of SO_2 in the fluids and the retrograde solubility of anhydrite.
iv) Epidote ± chlorite, representing nearly isochemical thermal metamorphism, is confined to discontinuous regions (tens to hundreds of metres across) that are surrounded by sericite + anhydrite + pyrite alteration.
v) Smectite is not detectable in bulk powders in the GIC, and kaolinite is only present as a minor constituent indicating the flow of acidic fluids at low temperatures was very limited.
vi) X-ray mapping of 18 samples indicated that heavy metal (Pb, Zn, As, Hg) phases are very scarce. These metals, almost certainly present in significant quantities, were steadily flushed through the system.
vii) Lateral thermal gradients were on the order of 500°C/km. Vertical thermal gradients in the centre of the system were probably even greater. Extreme thermal gradients and low confining pressures combined to localise precipitation of copper and gold.
viii) Alteration is explicable by a model of acid production/consumption in which magnetite precipitation in the core of the GIC generated abundant acid that caused phyllic alteration in the periphery.
ix) The limited overprint of the sericite + anhydrite + pyrite zone on the biotite + magnetite zone, minor development of kaolinite, and scarcity of trace metal phases, all indicate the hydrothermal system did not slowly wane, but instead shut down rather abruptly.

The Grasberg Cu-Au deposit is petrologically anomalous only in regard to grade and tonnage. The pervasive alteration (and vein) mineralogy of the Grasberg system is relatively simple compared to other copper porphyry systems because overprinting relationships are minor. The deviations from idealised models of porphyry copper deposits include the presence of andalusite in the core, the scarcity of smectite, and the minor overprint of the sericite + anhydrite + pyrite zone upon the biotite + magnetite zone.

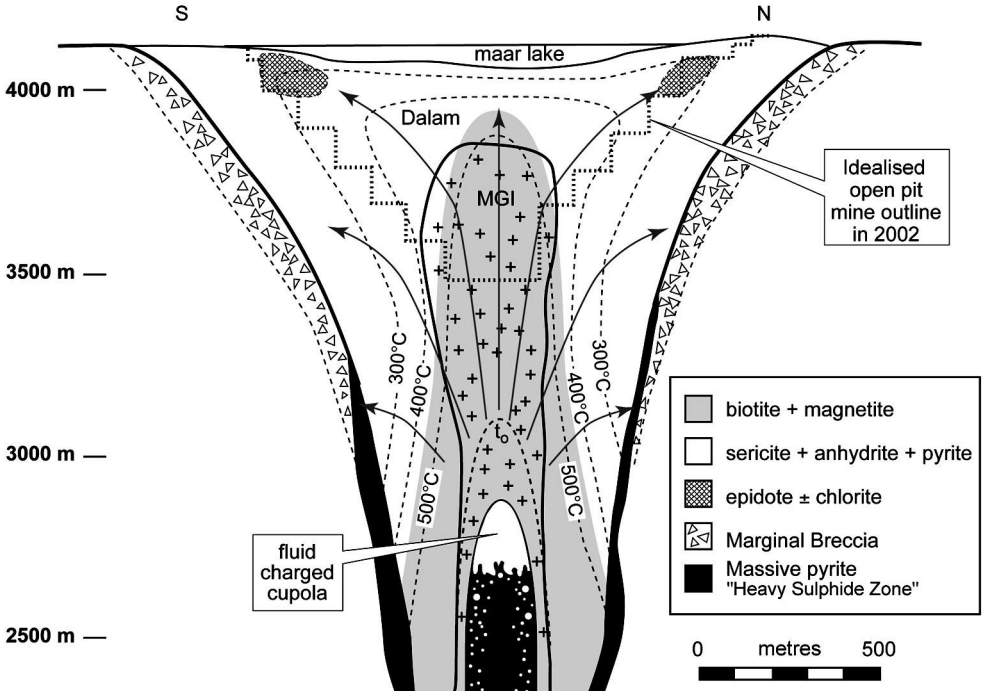

Figure 25: ***Interpretation of the Grasberg hydrothermal system.*** Magmatism in a maar-caldera. Pervasive hydrothermal alteration and ore mineralisation caused by the infiltration of magmatic fluids that emanate from the top of a fluid-charged cupola. When the system was active, the maar lake was a field of boiling halloysite clay mud pots.

The exceptional grade and tonnage of the Grasberg Cu-Au orebody is most likely accountable by a large steady flow up the centre of the system combined with extreme thermal gradients that focused the precipitation of copper and gold. The abrupt shutdown of the hydrothermal flow system indicates something profound occurred at depth. Most likely the area of fluid accumulation jumped to a different cupola – a phenomenon leading to the formation of major mineralisation elsewhere in the district.

Acknowledgements

From logistical to financial support, none of this work would have been possible without a large number of people from Freeport-McMoRan, Inc. and PT Freeport Indonesia: James R. Moffett, Dave Potter, George MacDonald, Wahyu Sunyoto, Sugeng Widodo, Noris Belluz, Keith Parris, Paul Warren, Clyde Leys, Herry Susanto, Chris Christenson, Bambang Irawan, Ben Coutts, Stephen Hughes, Nico Sambur, Aditya Pringgoprawiro, Boedijono, Yahul, and Bambang Antoro. A special thanks goes to Benyamin Sapiie. Ertsberg Project Contribution No. 24.

References

Arancibia, O.N. and Clark, A.H., 1996 - Early magnetite-amphibole-plagioclase alteration-mineralization in the Island Copper Porphyry copper-gold-molybdenum deposit, British Columbia: *Economic Geology*, v. 91, pp. 402-438.

Barnes, H.L., 1979 - Solubilities of ore minerals: *in* Barnes, H.L., (Ed.), Geochemistry of Hydrothermal Ore Deposits: *Wiley Interscience,* New York, 798p.

Beane, R.E., 1982 - Hydrothermal alteration in silicate rocks, southwestern North America: *in* Titley, S.R., (Ed.), Advances in Geology of the Porphyry Copper Deposits in Southwestern North America: *University of Arizona Press,* Tucson, pp. 117-137.

Beane, R.E. and Bodnar, R.J., 1995 - Hydrothermal fluids and hydrothermal alteration in porphyry copper deposits: *in*, Pierce, F.W. and Bolm, J.G., (Eds.), Porphyry Copper Deposits of the American Cordillera: *American Geological Society Digest* v. 20, pp. 83-93.

Beane, R.E. and Titley, S.R., 1981 - Porphyry copper deposits, part II, hydrothermal alteration and mineralization: *Economic Geology* 75th Anniversary Volume, pp. 235-269.

Berger, G. and Velde, B., 1992 - Chemical parameters controlling the propylitic and argillic alteration process: *European Journal of Mineralogy,* v. 4, pp. 1439-1454.

Blount, C.W. and Dickson, F.W., 1969 - The solubility of anhydrite ($CaSO_4$) in NaCl-H_2O from 100 to 450°C and 1 to 1000 bars: *Geochimica et Cosmochimica Acta,* v. 33, pp. 227-245.

Burnham, C.W., 1979 - Magmas and hydrothermal fluids: *in* Barnes, H.L., (Ed.), Geochemistry of Hydrothermal Ore Deposits, 2nd ed., *Wiley Interscience,* New York, pp. 71-136.

Burnham, C.W. and Ohmoto, H., 1980 - Late stage processes of felsic magmatism: *in* Ishihara, S. and Takenouchi, S., (Eds.), Granitic Magmatism and Related Mineralization: *Society of Mineralogy and Geology of Japan,* Special Issue 8, pp. 1-11.

Cloos, M., 2001, - Bubbling magma chambers, cupolas, and porphyry copper deposits: *International Geology Review,* v. 43, pp. 285-311.

Cloos, M. and Sapiie, B., 2005 - Porphyry copper deposits: Strike-slip faulting and throttling cupolas; Geological Society of America Abstracts with Programs, Vol. 37, No. 7, p. 97.

Creasey, S.C., 1966 - Hydrothermal alteration: *in* Titley, S.R. and Hicks, C.L., (Eds.), Geology of the porphyry copper deposits: Southwestern North America: *University of Arizona Press,* Tucson, pp. 51-74.

Dilles, J.H. and Einaudi, M.T., 1992 - Wall-rock alteration and hydrothermal flow paths about the Ann Mason porphyry copper deposit, Nevada-A 6 km vertical reconstruction: *Economic Geology,* v. 87, pp. 1963-2001.

Giggenbach, W. F., 1992 - Magma degassing and mineral deposition in hydrothermal systems along convergent plate boundaries: *Economic Geology,* v. 87, pp. 1927-1944.

Guilbert, J.M. and Park, C.F., 1985 - The Geology of Ore Deposits: *W.H. Freeman and Co.,* New York, 985p.

Gustafson, L.B. and Hunt, J.P., 1975 - The porphyry copper deposit at El Salvador, Chile: *Economic Geology,* v. 70, pp. 875-912.

Harris, A.C. and Golding, S.D., 2002 - New evidence of magmatic-fluid-related phyllic alteration: Implications for the genesis of porphyry Cu deposits: *Geology,* v. 30, pp. 335-338.

Harrison, J.S., 1999 - Hydrothermal alteration and fluid evolution of the Grasberg porphyry Cu-Au deposit, Irian Jaya, Indonesia: [M.S. Thesis]: *The University of Texas at Austin,* 205p.

He, S. and Morse, J.W., 1993 - Prediction of halite, gypsum and anhydrite solubility in natural brines under sub surface conditions: *Computers and Geosciences,* v. 19, pp. 1-22.

Hedenquist, J.W., Arribas, A. and Reynolds, T.J., 1998 - Evolution of a intrusion-centered hydrothermal system: Far Southeast Lepanto porphyry and epithermal Cu-Au deposits, Philippines: *Economic Geology,* v. 90, pp. 1506-1532.

Hedenquist, J.W. and Richards, J.P., 1998 - The influence of geochemical techniques on the development of genetic models for porphyry copper deposits: *in* Techniques in Hydrothermal Ore Deposits Geology: *Reviews in Economic Geology,* v. 10, pp. 235-256.

Hemley, J.J. and Jones, W.R., 1964 - Chemical aspects of hydrothermal alteration with emphasis on hydrogen metasomatism: *Economic Geology,* v. 59, pp. 538-569.

Holland, H.D., 1965 - Some applications of thermochemical data to problems of ore deposits, II. Mineral

assemblages and the composition of ore-forming fluids: *Economic Geology,* v. 60, pp. 1101-1166.

Holland, H.D. and Malinin, S.D., 1979 - The solubility and occurrence of non-ore minerals: *in* Barnes, H.L., (Ed.), Geochemistry of Hydrothermal Ore Deposits, 2nd ed.: *Wiley Interscience,* New York, pp. 461-508.

Lambert, C.A., 2000 - Subsurface meso-scale structural geology of the Kucing Liar and Amole Drifts and petrology of the Heavy Sulfide Zone, South Grasberg Igneous Complex, Irian Jaya, Indonesia: [M.S. Thesis]: *The University of Texas at Austin,* 253p.

Lowell, J.D., 1995 - The Richard and Coutright era and why some exploration programs are successful: *in* Pierce, F.W. and Bolm, J.G., (Eds.), Porphyry Copper Deposits of the American Cordillera: *American Geological Society Digest* v. 20, pp. 3-5.

Lowell, J.D. and Guilbert, J.M., 1970 - Lateral and vertical alteration-mineralization zoning in porphyry ore deposits: *Economic Geology,* v. 65, pp. 373-408.

MacDonald, G.D. and Arnold, L.C., 1994 - Geological and geochemical zoning of the Grasberg Igneous Complex, Irian Jaya, Indonesia: *Journal of Geochemical Exploration,* v. 50, pp. 143-178.

Manske, S.L. and Paul, A.H., 2002 - Geology of a major new porphyry copper center in the Superior (Pioneer) District, Arizona: *Economic Geology,* v. 97, pp. 197-220.

McMahon, T.P., 1994a - Pliocene intrusions in the Gunung Bijih (Ertsberg) Mining District, Irian Jaya, Indonesia: Petrography and mineral chemistry: *International Geology Reviews,* v. 36, pp. 820-849.

McMahon, T.P., 1994b - Pliocene intrusions in the Ertsberg (Gunung Bijih) Mining District, Irian Jaya, Indonesia: Petrography, geochemistry and tectonic setting [Ph.D. Dissertation]: *The University of Texas at Austin,* 298p.

McMahon, T.P., 1994c - Pliocene intrusions in the Gunung Bijih (Ertsberg) Mining District, Irian Jaya, Indonesia: Major- and trace-element chemistry: *International Geology Review,* v. 36, pp. 925-946.

Moller, N., 1988 - The prediction of mineral solubilities in natural waters: A chemical equilibrium model for the Na-Ca-Cl-SO_4-H_2O system, to high temperature and concentration: *Geochimica et Cosmochimica Acta,* v. 52, pp. 821-837.

Paterson, J. T., 2004 - Magmatic and pervasive hydrothermal mineralogy of the Grasberg porphyry Cu-Au deposit (west New Guinea): [M.S. Thesis]: *The University of Texas at Austin,* 332p.

Pennington, J. and Kavalieris, I., 1997 - New advances in the understanding of the Grasberg copper-gold porphyry system, Irian Jaya, Indonesia: Pacific Treasure Trove - Copper-Gold Deposits of the Pacific Rim: *Annual Convention and Trade Show of the Prospectors and Developers Association of Canada,* pp. 79-97.

Penniston-Dorland, S., 1997 - Veins and alteration envelopes in the Grasberg Igneous Complex, Gunung Bijih (Ertsberg) District, Irian Jaya, Indonesia: [M.S. Thesis]: *The University of Texas at Austin,* 402p.

Penniston-Dorland, S., 2001 - Illumination of vein quartz textures in a porphyry copper ore deposit using scanned cathodoluminescence: Grasberg Igneous Complex, Irian Jaya, Indonesia: *American Mineralogist,* v. 86, pp. 652-666

Pollard, P.J. and Taylor, R.G., 2002 - Paragenesis of the Grasberg Cu-Au deposit, Irian Jaya, Indonesia: Results from logging section 13: *Mineralium Deposita,* v. 37, pp. 117-136.

Reed, M.H., 1997 - Hydrothermal alteration and its relationship to ore fluid composition: *in* Barnes, H.L., (Ed.), Geochemistry of Hydrothermal Ore Deposits, 2nd ed.: *Wiley Interscience,* New York, 798p.

Richards, J.P., Ronacher, E. and Johnston, M., 1998 - New mineralization styles at the Porgera gold deposit, Papua New Guinea: *Geological Society of America,* Abstracts with Programs, v. 30, pp 302.

Rose, A.W. and Burt, D.W., 1979 - Hydrothermal Alteration: *in* Barnes, H.L., (Ed.), Geochemistry of Hydrothermal Ore Deposits, 2nd ed.: *Wiley Interscience,* New York, 798p.

Rubright, R.D. and Hart, O.J., 1968 - Non-porphyry ores of the Bingham district, Utah: *in* Ore Deposits of the United States, 1933-1967: v.1, pp. 886-908.

Sales, R.H. and Meyer, C., 1950 - Interpretation of wall-rock alteration at Butte-Montana: *Colorado School of Mines* Quarterly, v. 45, pp. 261-273.

Sapiie, B., 1988 - Strike-slip faulting, breccia formation and porphyry Cu-Au mineralization in the Gunung Bijih (Ertsberg) Mining District, Irian Jaya, Indonesia: [Ph.D. Dissertation]: *The University of Texas at Austin,* 304p.

Taylor, H.P., 1974 - The application of oxygen and hydrothermal isotope studies to problems of hydrothermal alteration and ore deposition: *Economic Geology,* v. 69, p. 229-302.

Thorez, J., 1976 - Practical Identification of Clay Minerals: Belgium, 90p.

Titley, S.R., 1982 - The style and progress of mineralization and alteration in porphyry copper systems, American southwest: *in* Titley, S.R., (Ed.), Advances in Geology of the Porphyry Copper Deposits in Southwestern North America: *University of Arizona Press,* Tucson, pp. 117-137.

Ulrich, T., Guenther, D. and Heinrich, C.A., 1999 - Gold concentrations of magmatic brines and the metal budget of porphyry copper deposits: *Nature* (London), v. 399, pp. 676-679.

Ulrich, T. and Heinrich, C.A., 2001 - Geology and alteration geochemistry of the porphyry Cu-Au deposit at Bajo de la Alumbrera, Argentina: *Economic Geology,* v. 96, pp. 1719-1742.

Van Nort, S.D., Atwood, G.W., Collinson, T.B., Flint, D.C. and Potter, D.R., 1991 - Geology and mineralization of the Grasberg copper-gold deposit: *Mining Engineering,* v. 43, pp. 300-303.

Williams, S.A. and Forrester, J.D., 1995 - Characteristics of porphyry copper deposits: *in* Pierce, F.W., and Bolm, J.G., (Eds.), Porphyry Copper Deposits of the American Cordillera: *American Geological Society Digest* v. 20, pp. 21-34.

Wood, S.A., 1998 - Calculation of activity-activity and log fO_2-pH diagrams: *in* Techniques in Hydrothermal Ore Deposits Geology: *Reviews in Economic Geology,* v. 10, pp. 81-96.

Wood, S.A. and Samson, I.M., 1998 - Solubility of ore minerals and complexation of ore metals in hydrothermal solutions: *in* Techniques in Hydrothermal Ore Deposits Geology: *Reviews in Economic Geology,* v. 10, pp. 33-80.

Yavuz, F. and Oztas, T., 1997 - BIOTERM-A program for evaluating and plotting microprobe analyses of biotite from barren and mineralized magmatic suites: *Computers and Geosciences,* v. 23, pp. 897-907.